The role of PerR in Group B *Streptococcus* regulation of peroxide and iron stress

A Thesis Presented for the

Master of Science

Degree

The University of Tennessee, Knoxville

Stephen W Lumsdaine

May 2025

Dedication

I would like to dedicate this work to all the people that support the progression of science, especially in areas that strive to better the condition of the most vulnerable in society.

Acknowledgements

I would like to give my everlasting thanks to my fantastic advisor Lindsey Burcham, and for her tireless support of me as both a scientist and a person. Her direction has unquestionably made me a better scientist, and her leadership has made me a better person.

I would like to thank the other members of the Burcham lab, Abbey, Tammana, Emily, Ryan, Natalie, and yes even Jéssica. They have made the lab a place where both science and fun can flourish, and where we can support each other through whatever problems school or research may throw at us.

I am thankful to my committee members, Dr. Erik Zinser and Dr. Andrew Monteith, for their support and advice throughout my study, and for being willing to meet every 6 months rather than once a year to better inform and guide my project. Their advice was instrumental, and I always came out of committee meetings feeling like they wanted me to succeed.

I would also like to thank Dr. Todd Reynolds and Dr. Andy Wagner and the rest of the Reynolds lab; Elise, Jordan, Aeric, Mikayla and Ainsley. As a graduate student I have realized the investment and time it takes to provide quality mentorship to an undergraduate, and that is exactly what Andy and Todd provided to me.

I am also very appreciative of all the friendship and support throughout the microbiology department by students, staff, and professors, and for my friends and family outside of school. I have been blessed to know so many amazing people. I am especially thankful to Morgan, Dr. Tim Sparer and the Sparer lab for their help with blood draws and blood related assays.

A special thanks to my parents and all of my siblings, who I have been lucky enough to see regularly throughout my education. I appreciate their friendship and love and support, and look forward to seeing where life takes all of them.

Above all, I am thankful for the Son Jesus Christ; for the truth of his Word and the example of his life; for his steadfast obedience, by which he overcame temptation; for his dying, through which he overcame death; and for his rising to life again, in which we are raised to the life of His kingdom.

Abstract

Streptococcus agalactiae, also known as Group B *Streptococcus* (GBS), is a Gram-positive facultative anaerobe that generally persists in the gut and reproductive tract, and can become opportunistically pathogenic in immunocompromised hosts. PerR, or the peroxide responsive repressor, is a transcriptional repressor identified in a high throughput murine vaginal colonization transposon mutagenesis experiment as important for persistence in that environment and has not previously been characterized in GBS. Here we have investigated the role of PerR to better understand the mechanisms involved in the GBS response to reactive oxygen species (ROS) and iron stress. Characterizing the role of PerR in GBS has increased our understanding of how this catalase negative organism responds to ROS and has provided insight into how the ROS response and iron homeostasis may overlap. We constructed *perR* deletion strains and showed that PerR serves as a regulator of the peroxide stress response, and deletion strains show increased resistance to hydrogen peroxide. In a murine model of GBS vaginal colonization, *perR* deletion strains also showed a modest decreased colonization persistence compared to WT strains in CD-1 mice, thought this phenotype was not consistent across different mouse backgrounds. PerR was also shown to play a role in iron regulation and homeostasis, as a deletion strain shows both increased sensitivity to iron chelation. QRT-PCR was also used to identify several genes involved in iron homeostasis, *fetB and VIT*, that are upregulated in a *perR* mutant background and may fall within the PerR regulon. Due to the role of GBS as an opportunistic pathogen in systemic disease, we investigated the virulence of the *perR* mutant in a murine model of systemic disease. In this model, the mutant strain showed significantly decreased virulence compared to WT strains. Overall, we have shown that GBS PerR functions as an important regulator, contributing to expression of genes involved in peroxide stress, iron

homeostasis, as well as genes associated with virulence and a previously unstudied prophage element.

Table of Contents

Chapter 1: Literature Review 1

Streptococcus agalactiae prevalence 1

GBS virulence 2

Reactive Oxygen Species 5

Iron Metabolism in GBS 7

PerR 9

Chapter 2: Physiological Impact of PerR 12

Introduction 12

Methods 12

Bacterial strains and generation of mutants and complement strains used in this work 12

RNA sequencing and analysis and Quantitative reverse transcriptase PCR (RT-qPCR) 13

Oxidative stress survival and breakdown 14

Iron Assays 15

Sequence Alignment and Analysis 15

Results 16

Hydrogen Peroxide Breakdown 15

PerR structure 18

Strain growth and response to H_2O_2 and iron chelation 18

RNAseq and RT-qPCR 24

Chapter 3: Role of PerR in Colonization and Disease 29

Introduction 29

Methods 29

Murine Models of Vaginal Colonization and Systemic Infection....29
Vaginal Cell Assays....31
Growth in Human Blood....31
Results....32
Murine Model of Vaginal Colonization....32
Vaginal Cell Assays....37
Murine Model of Systemic Disease....37
Growth in Blood....40
Chapter 4: Discussion....45
Future Directions....52
References....54
Appendix....72
Vita....78

List of Tables

Table 1: RNAseq identified differentially expressed genes Δ*perR* vs WT 26

Table 2: Primer List 74

Table 3: Predicted PerR Regulated Genes 75

List of Figures

Figure 1: Breakdown of H_2O_2 by GBS bacterial culture and supernatant 17

Figure 2: *Streptococcus agalactiae* PerR structure and binding.....19

Figure 3: Growth curves and colony counts of GBS CJB111 strains in THB and SVF.....21

Figure 4: Growth curves and plate counts of GBS A909 strains in SVF 22

Figure 5: Differential survival of GBS strains with H_2O_2 in complex media.....23

Figure 6: Impact of iron chelation with 2,2-bipyridyl on strain growth 25

Figure 7: qPCR analysis of differential gene expression in *ΔperR* strains 27

Figure 8: A909 murine vaginal colonization model in 5-week C57BL/6N.....33

Figure 9: A909 murine vaginal colonization model in 9-week old C57BL/6J.....34

Figure 10: CJB111 murine vaginal colonization model in C57BL/6 35

Figure 11: CJB111 murine vaginal colonization model in CD-1 mice 36

Figure 12: GBS A909 and CJB111 adhesion to vaginal epithelial cells 38

Figure 13: A909 murine model of systemic disease in C57BL/6.....39

Figure 14: CJB111 murine model of systemic disease in C57BL/6 41

Figure 15: CJB111 murine model of systemic disease in neutrophil depleted C57/BL6.....42

Figure 16: Survival of A909 and CJB111 strains in human blood.....43

Figure 17: Proposed perR regulon in Group B streptococcus 49

Figure 18: Comparative growth of GBS strains with and without pABG5 plasmid vector 72

Figure 19: S100A8/A9 ELISA for conformation of C57BL/6 neutrophil depletion.....73

Chapter 1: Literature Review

Streptococcus agalactiae prevalence

Streptococcus agalactiae, also known as Group B *Streptococcus* (GBS), is a Gram-positive, beta-hemolytic facultative anaerobe that colonizes the human gut and reproductive tract as a commensal species. However, in certain high-risk populations such as pregnant people, neonates, elderly and immunocompromised individuals it can opportunistically cause invasive disease (Shane 2019). GBS is traditionally classified by the capsular serotype with 10 known serotypes, Ia, Ib, II, III, IV, V, VI, VII, VIII, and IX, though the first six serotypes make up ~95% of all isolates (Bianchi-Jassir 2020). Serotypes Ia and III are most commonly associated with maternal systemic disease, followed by V, Ib and II. However, serotype prevalence and colonization prevalence can very broadly across location and ethnicity.

One of the primary areas of medical relevance for GBS research revolves around maternal-fetal health. Globally prevalence of GBS rectovaginal colonization in women is 18%, though that can vary significantly by country and ethnic background, with examples of 35% of women colonized in the Caribbean, or 11% colonized in northern Asia (Russel 2017). GBS typically exists as a commensal organism within the reproductive tract, and during pregnancy it is associated with numerous adverse events or conditions including preterm premature rupture of membranes, preterm labor, chorioamnionitis, endometritis, pyelonephritis, peripartum bacteremia, and neonatal disease (Cape 2013, Sachdeva 2024, Morgan 2024). To minimize the risk of vertical transmission of GBS to the infant during birth, many countries have implemented prenatal screening to test for rectovaginal presence of GBS through two primary screening approaches. Risk-based prophylaxis (RBP) identifies women with specific risk factors for the development of GBS disease and intervenes with antibiotic treatment during labor. These risk

factors include ethnicity, young maternal age, exposure to HIV, or those who have experienced premature birth, low birth weight, rupture of membranes (Berardi 2021). Screening-based prophylaxis (SBP) screens pregnant individuals for GBS colonization between weeks 35-37 gestation and recommends GBS-positive individuals receive antibiotics during labor. In a longitudinal study monitoring cases of neonatal early-onset GBS infections in Nordic countries, universal screening was associated with a 58% reduction in early-onset disease while risk-based approaches were associated with an 11% decrease (Björklund 2024). However, many low-to-middle income countries do not have standards for GBS screening or have limited resources and minimal application of these standards.

GBS Virulence

In infants, GBS infection is usually divided between early-onset disease (EOD) and late onset disease (LOD). EOD is categorized by clinical disease presentation within 0-6 days of birth, while later presentation, occurring days 7-89 after birth are considered LOD (Lawn, 2022). In GBS colonized mothers, transmission to newborns resulting in EOD most commonly occurs during labor or preterm premature rupture of membranes (PPROM). In the absence of antibiotic prophylaxis, 1-2% of newborns will develop EOD (American College of Obstetricians and Gynecologists, 2020). EOD is diagnosed through isolation of GBS from a normally sterile site of the infant, and could present as sepsis, pneumonia or occasionally meningitis, and symptoms are most commonly observed within the first two days following birth. GBS maternal colonization can also result in GBS colonization of the infant gut and may impact infant microbiome structure, or transition to LOD (Cassidy-Bushrow 2017, Li, 2024). LOD is more often associated with bacteremia, pneumonia and meningitis. However, unlike the transmission route of EOD, the mechanism of infection for LOD is still unclear. Intrapartum antibiotic prophylaxis (IAP) does

successfully reduce rates of EOD but only impacts onset and severity of LOD, not rate of disease. This indicates that transmission from a GBS colonized mother before or during birth remains one vector for LOD, but transmission post-labor from caregivers or infected breastmilk are also considered potential causes (Berardi 2021**)**.

Clinical genomic studies and laboratory research have identified a broad spectrum of genes in GBS that contribute to vaginal colonization and persistence, as well as neonatal disease. Sialic acid capsular polysaccharide, the terminal sugar residue in the polysaccharide capsule of all GBS serotypes, has been well characterized as a virulence factor in GBS. Differences in capsule polysaccharide structure is the source of GBS differentiation into 10 different serotypes. The capsule itself is formed of a combination of glucose, galactose, N-acetylglucosamine, rhamnose, and sialic acid in all serotypes, though the chaining and structure of these components is organized differently across different serotypes (Cieslewicz 2005). As capsule is at the front line of interaction with the host, it has been implicated as a major factor in GBS immune evasion and survival (Carlin 2009, Chang 2014). Capsule differences across serotype are also thought to be at least partially responsible for different clinical outcomes. Serotypes Ia, Ib, II and V have been observed to be less associated with LOD compared to EOD. Serotype III however showed higher frequency in LOD than EOD, as serotype III isolates are responsible for the majority of LOD cases (Chaguza 2022).

Two-component systems are a primary method by which bacteria sense and respond to environmental change. GBS expresses 21 two-component systems, though many have not been well characterized (Faralla 2014). Several of these systems, including CovR/S, SaeR/S, CiaR/H, LiaR/H, RgfA/C, and HssR/S have been identified as regulators of virulence in both in vivo and in vitro models (Armistead 2019). The CovR/S system is the most broadly studied and has been

shown to regulate the β-hemolysin/cytolysin toxin, adhesins, and a wide range of other virulence factors in GBS. Though CovR/S is highly conserved within streptococcus species, its regulation can show significant differences even across different GBS strains (Jiang 2008). SaeR/S has also been shown to positively regulate factors important for vaginal colonization and persistence, like the plasminogen binding adhesin PbsP and the Group B vaginal adhesion protein BvaP (Cook 2018, Cook 2022).

PbsP is a plasminogen binding surface protein that contributes both GBS colonization of the vaginal environment, as well as bacterial dissemination and invasion of the brain (Cook 2018, Buscetta 2016, Lentini 2018). GBS contains many surface anchored or secreted proteins that impact bacterial adhesion. All GBS clinical isolates encode for at least one of two major pilus islands, labeled PI-1 and PI-2, with PI-2 showing two further subtypes, 2a and 2b, and pilus has been shown to play an important role in immune modulation, vaginal colonization, mucosal attachment, and meningeal disease (Margarit 2009, Banerjee 2011, Burcham 2022). GBS uses a broad range of additional adhesions, including serine rich repeat proteins and fibrinogen binding proteins, to persist in numerous host niches (Megli 2025).

Another important virulence factor in GBS is β-hemolysin/cytolysin toxin (βH/C), one of several toxins encoded by GBS (Megli 2025). βH/C is the primary cause of GBS's characteristic zones of clearing on blood agar, and acts both to form pores in eukaryotic cell barriers and to enhance survival from host immune cell damage. βH/C and its associated pigment are important for virulence in numerous host niches, as well as in immune modulation (Liu 2004, Randis 2014, Doran 2003, Bebien 2012). The *cyl* gene cluster is responsible for encoding βH/C as well as GBS pigment, and is regulated by the CovR/S two-component system (Rosa-Fraile 2014).

While much of GBS clinical relevance is in relation to maternal-fetal health, it can also cause disease in non-pregnant populations, particularly the elderly or those with chronic medical conditions. One study identified GBS in 100 per 100,000 hospitalizations among those greater than 65 years of age, though non-invasive disease (skin and soft tissue, urinary tract and respiratory tract infections) was almost four times more common than invasive disease (bacteremia, necrotizing fasciitis, meningitis or cardiovascular disease). However, it should be noted that presence of GBS did not necessarily indicate it was the cause of hospitalization, and the rate of invasive GBS in the 65+ population was 25 per 100,000 hospitalizations (McLaughlin 2021). Chronic disease also increased the likelihood of invasive GBS disease, with diabetes the most prevalent underlying condition especially in context of soft tissue infections (Skoff 2009).

Reactive Oxygen Species

Reactive oxygen species (ROS) are reactive forms of oxygen present in almost all environments, most commonly superoxide (O_2^-), hydroxyl radicals ($HO^\bullet$), hydrogen peroxide (H_2O_2), and singlet oxygen ($^1O_2^-$). ROS are produced endogenously as natural byproducts of cellular aerobic metabolism and various catalytic and enzymatic reactions, as well as exogenously by ionizing and UV radiation and numerous pollutants. They are also used at low levels in numerous mechanisms for cell signaling in the form of H_2O_2 mediate oxidation of protein-cysteine thiols, but uncontrolled can deal direct damage to DNA, lipids and proteins through uncontrolled oxidation (Veal 2024). ROS are produced by the host immune system, largely due to the activity of NADPH oxidase, and contribute to phagocyte microbial killing (Nathan 2013**)**. As such, almost all life has developed mechanisms for facilitating the breakdown of ROS, and microbes are no different. While different species vary broadly in how they respond to ROS induced stress, systems like superoxide dismutase, catalase, thioredoxins, and

glutathione reductases are common mechanisms for responding to ROS induced stress. Systems involved in the management of iron homeostasis are also often important for combatting ROS, as free iron has the potential to induce redox damage through the Fenton reaction (Li 2021**)**. Within the vaginal tract ROS presence has not been precisely characterized, though ROS have been identified as contributing factors to numerous disease morphologies relevant to female reproductive health (Lu 2018). Increased ROS levels are associated with endometriosis, polycystic ovary syndrome, fertility issues and numerous pregnancy complications (Jackson 2005, Palacio 2006, Watson 1998). While mitochondrial ROS production, lifestyle factors, hormone and nutrient deficiencies are the major drivers of ROS related disease in the female reproductive tract, nonspecific vaginitis has also been associated with higher levels of ROS and lower levels of catalase activity in the vaginal tract (Chen 2015).

There has been significant work in studying the impact of hydrogen peroxide (H_2O_2) as an antimicrobial factor in the vaginal microbiome. Some studies have observed that increased presence of H_2O_2 producing lactobacillus species, such as *L. crispatus*, *L. gasseri*, *L. vaginalis and L. jensenii* are associated with decreased risk of preterm birth and bacterial vaginosis, while species that do not produce H_2O_2, like *L. iners*, are not (Wilks 2004, Vallor 2001, Cherpes 2008). Additionally, numerous species associated with or causative of dysbiosis and infection are sensitive to H_2O_2 within concentrations that have been produced by some lactobacillus species *in vitro* (Strus, 2006). However, this effect has not been demonstrated under *in vivo* conditions. Current literature indicates that concentrations of H_2O_2 produced by lactobacillus in vaginal fluid under anaerobic conditions is 23 μM ± 5 μM, a 100-fold decrease from what was observed aerobically in rich aerated media (O'Hanlon, 2010). Conditions in the female reproductive tract are primarily anaerobic, which is not conducive to the production of H_2O_2. While certain factors,

like tampon insertion, sexual arousal and vaginal intercourse may cause shifts away from a hypoxic environment, oxygen may still lack the abundance required for biologically relevant inhibition by H_2O_2 production as a continual mechanism of inhibition by *lactobacillus*. Cervicovaginal fluid has also been shown to be inhibitory to the production of H_2O_2, which combined with the presence of catalase and other peroxidases in the reproductive tract indicates H_2O_2 does not play the primary role as an inhibitory factor in the vaginal microbiome, though it may still be situationally relevant (O'Hanlon, 2013).

One hallmark of organisms of the genus *Streptococcus* is their lack of catalase, the primary enzyme that catalyzes decay of H_2O_2. This means these species require alternate mechanisms for managing peroxide stress. Within GBS, response to ROS stressors is broadly uncharacterized, though GBS is known to encode a manganese bound superoxide dismutase (*SodA*), *AhpC,* an NADH peroxidase *npx,* a thiol peroxidase *tpx*, and a glutathione reductase (Korir 2018). Several other systems, including manganese transporters *mtsA and mntH* (Shabayek 2016, Burcham 2022) and the *bceR* two-component system, show increased ROS sensitivity when deleted.

Iron Metabolism in GBS

Iron is an important cofactor for a broad spectrum of enzymes used in bacterial metabolism, and it is estimated at least 10^{-8} mol/L of iron is required for bacterial growth (Ge 2009). However, as mentioned previously, too much free iron can result in ROS stress through the Fenton reaction, so maintaining the balance of iron homeostasis is vital for bacterial function. In a human host environment iron is generally a bioavailably limited nutrient due to host sequestration. This is conducted by a number of host proteins; including transferrins which bind with high affinity to two iron molecules, ferratin which act as the primary iron storage molecule

in animals, and numerous immune associated proteins like lipocalin-2 and calprotectin. (Ullah 2023). Due to these mechanisms by the host to limit iron access, bacterial iron acquisition and scavenging is a critical factor for virulence and survival within the host. GBS encodes several characterized systems that may contribute to iron acquisition, including MtsABC, a Fe^{2+}/Mn^{2+} ABC transporter, and FhuCDBG, a siderophore dependent iron transporter (Bray 2009, Clancy 2005). It is worth noting that while the MtsABC transporter has been shown to transport iron in GAS, and that iron can regulate its expression in GBS, it has not been directly demonstrated as an iron transporter within GBS (Bray 2009, Sun 2008, Burcham 2022).

Within a human host, heme is one of the most abundant sources of iron, especially in the blood. Heme acquisition and transport systems have been characterized in many streptococcal species, but not in GBS. However, as GBS lacks heme synthesis pathways, it must rely on scavenging it from the environment (Joubert 2017). Additionally, heme is required for GBS to conduct respiration metabolism rather than fermentation. This heme and menaquinone dependent switch to respiration rather than fermentative metabolism has been shown to contribute to GBS virulence (Yamamoto 2005). Numerous genes involved in heme homeostasis have been characterized within GBS, though complete import systems for heme scavenging are yet unidentified. The alkyl hydroperoxide reductase AhpC has been found to bind heme and participate in storage and intracellular availability within GBS. This gene has also been identified being involved in the response to H_2O_2 stress in *Streptococcus pyogenes*, or Group A *Streptococcus* (GAS) (Lechardeur 2010). Homologs of the HrtBA heme efflux transporter, HssR (heme sensing response regulator), and HssS (heme sensing histidine kinase) of *Staphylococcus aureus* have been identified on one operon in GBS and contribute to heme sensing and heme homeostasis. During invasion of a human host, GBS may encounter heme rich conditions in the

organs or blood and maintaining mechanisms to reduce heme toxicity are vital for successful virulence (Joubert 2017). Two additional operons, encoded by *pefAB* and *pefRCD,* form exporters that transport the heme precursor protoporphyrin IX and heme, that are under the regulation of the PefR repressor (Fernandez 2010). In a *pefR* mutant background, the constant heme export results in a failure to maintain intracellular heme levels and results in respiration defects (Fernandez 2010).

PerR

As H_2O_2 produced by both internal and external factors is a stressor encountered by most bacteria, many different species have evolved mechanisms for regulating the response to that stress (Sen 2021). Many Gram-negative bacteria, like *Escherichia coli* and *Salmonella enterica* encode the transcription factor OxyR, which acts as a master regulator of peroxide response. In Gram-positive species, PerR is more common, acting as a repressive regulator within *Bacillus, Staphylococcus* and *Streptococcus* species (Li 2021). Within most species that utilize PerR as a major regulator of the H_2O_2 stress response, catalase is consistently within the regulon of PerR (Ji 2015, Fuangthong 2002, Palyada 2009, Seixas 2025). However, as streptococcal species are catalase negative, understanding the function and role of PerR within ROS stress and homeostasis is especially interesting.

While *perR* has not been characterized within GBS, it has been investigated in *Streptococcus pyogenes, Streptococcus suis,* and *Streptococcus mutans,* as well as non-streptococcal Gram-positives like *Staphylococcus aureus,* and *Bacillus subtilis* (Herbig 2002). It is a metalloregulator within the same family as the ferric uptake regulator (FUR). Fur family proteins traditionally act as metal bound repressors that modulate metal homeostasis, and have been identified as regulators for zinc, manganese, nickel, and primarily, iron (Lee 2007).

The binding of PerR as a repressive regulatory mechanism is typically driven by a sequence element termed the *per* box, similar in nature to the *fur* box observed in FUR regulation within many species (Baichoo 2003, Troxell 2013). This PerR binding motif, usually represented upstream of the -10 or -35 genes in the promoter of a regulated gene, is a conserved inverted repeat that functions as the primary binding site for repressive regulation by the PerR protein. From a structural standpoint, PerR contains two metal binding sites critical to its function. PerR protein from *B. subtilus,* GAS, and *S. aureus* all exhibit a structural zinc binding site, as well as a regulatory metal binding site. The regulatory binding site allows PerR to bind to a metal ion cofactor, and has high affinity for both iron and manganese binding (Makthal 2013, Ricci 2002, Ji 2015). While some other metals have also demonstrated binding affinity for PerR, like nickel and cobalt, iron and manganese are thought to be the primary metal cofactors (Herbig, 2001).

It has been shown in *B. subtilus*, perhaps the best studied system of PerR regulation, that oxidation of PerR at its metal binding regulatory site induces a conformational change. This change then results in protein separation from bound DNA, and de-repression of the target gene. (Traoré 2009, Lee 2007). This oxidation that initiates de-repression can be caused by H_2O_2, allowing a rapid response of PerR regulated peroxide response genes in the advent of H_2O_2 stress. While binding of regulatory metal is not required for PerR binding to the *per* box, it does result in higher affinity binding to DNA and is required for effective sensing of H_2O_2 (Makthal 2013).

In *B. subtilus* certain genes within the PerR regulon, including catalase (*KatA*), alkyl hydroperoxide (*AhpC*), iron sequestration DNA-binding protein MrgA, and *zosA*, have been well established as important for *B. subtilus* to respond to H_2O_2 stress (Helmann 2003, Martínez

2024). In GAS, while a *perR* mutant results in increase resistance to H_2O_2, PerR seems to regulate primarily DNA repair and iron homeostasis genes, and direct peroxide breakdown genes like *ahpC* or glutathione peroxidase (*gpoA*) are regulated in a PerR independent manner (Grifanti 2011, King 2000). A *perR* mutant GAS strain was demonstrated to show decreased virulence in a murine model of systemic infection (Ricci 2002).

Chapter 2: Physiological Impact of PerR

Introduction

Given the clinical relevance of GBS, it is important to continue to identify what factors contribute to its function as an opportunistic pathogen, both to help identify potential targets for drugs and vaccines and to better understand what treatment methods best apply in what conditions. Previous work to better characterize the genetic factors that contribute to vaginal colonization and persistence was done by conducting a murine vaginal colonization model using a pooled GBS mariner transposon (Krmit) mutant library (Burcham 2022). Using this method, Tnseq was conducted on tissue samples and vaginal swabs to identify over and under-represented mutations three days following murine colonization. The transposon mutants identified as differentially represented included a number of different genes involved in metal homeostasis and reactive oxygen species response, including *mtsA, mtsR, perR, fhuD, gorA, tpx,* and *soda* (Burcham 2022). Of these genes, *perR* was selected as the target of this study, as many of the mechanisms of ROS response in catalase-negative GBS are still uncharacterized. As *perR* generally acts as a regulator, characterizing its regulon and understanding its function will help clarify the ROS response in GBS. Additionally, while *perR* is a metalloregulator of the Fur family (Sevilla 2021), *perR* is the closest Fur homolog in GBS. Because of this we hypothesize that *perR* is functioning as both a H_2O_2 response regulator and a regulator of iron homeostasis.

Methods

Bacterial Strains and Generation of Mutant and Complement Strains Used in this Work

Streptococcus agalactiae (GBS) isolate A909 (serotype Ia) and isolate CJB111 (serotype V) and mutant strains A909Δ*perR* and CJB111Δ*perR*, as well as complement strains, A909Δ*perR*+pABG5:*perR* and CJB111Δ*perR*+pABG5:*perR*, were grown in Todd Hewitt Broth

(THB) aerobically at 37°C without agitation. Mutant strains were generated using techniques described previously (Spencer 2019). Briefly, ~1 kilobase 5' and 3' genomic regions flanking the *perR* gene were amplified via PCR, and fused together flanking a kanamycin resistance cassette and fused with a pHY304 plasmid vector at a 1:1 ratio using the New England Biolabs HiFi DNA assembly kit. Primers flanking the pHY304 multiple cloning site were used to confirm the presence of the insert within the plasmid vector. The completed plasmid was transformed into chemically component *Escherichia coli* MC1061 and plated on LB agar, selecting for transformants with erythromycin. The plasmid was then purified and electroporated into the A909 and CJB111 strains and plated on Todd Hewitt agar (THA) using erythromycin selection (500 µg/mL). The plasmid was integrated into and subsequently recombined out of the genome using the temperature sensitive nature of the plasmid, resulting in the replacement of the *perR* gene with the kanamycin resistance cassette, monitoring for erythromycin (5 µg/mL) kanamycin (50 µg/mL) resistance. Complement strains were constructed using the pABG5 expression plasmid as an empty vector or pABG5 engineered to express the *perR* gene and were electroporated into GBS WT and Δ*perR* strains and selected for using a kanamycin (500 µg/mL) (Granok 2000). Mutants were confirmed using PCR amplification of flanking regions, where a mutant strain showed larger PCR bands than the WT given the replacement of *perR* (~500kb) with the kanamycin resistance cassette (~1000kb), and whole genome sequencing.

RNA Sequencing and Analysis and Quantitative reverse transcriptase PCR (RT-qPCR)

For RNA sequencing, A909 GBS WT and Δ*perR* mutant strains were grown overnight in THB, and inoculated(1:10) into fresh media to mid-logarithmic phase in synthetic vaginal fluid (SVF), and then incubated for 3 hours in SVF with no treatment, 500 µM H_2O_2, or 500 µM 2,2-bipyridyl. Following incubation, bacteria were centrifuged at 10000 x g for 5 minutes, and RNA

was extracted (Macherey-Nagel). Total RNA samples were prepped for sequencing using a Zymo-seq RiboFree total RNA Library Kit (Zymo Research). Following RNA extraction, cDNA was synthesized using reverse transcription, and then ribosomal RNA was removed using RiboFree universal depletion. P7 and P5 adapter caps were then ligated to DNA, which was then amplified, barcoded and purified using MagBeads. Samples were then sequenced by Illumina sequencing at the University of Tennessee Knoxville Genomics core. General analysis was conducted by Z. Burcham lab at UTK, involving read quality control, followed by trimming, alignment, read counts and differential gene expression analysis.

For RT-qPCR, CJB111 WT/pABG5 EV, Δ*perR*/pABG5 EV, and Δ*perR*/pABG5:*perR* strains were grown overnight in THB. They were then inoculated(1:10) into fresh untreated THB media, THB with 150 µM H_2O_2, or THB with 500 µM 2,2-bipyridyl. Cultures were then grown to an OD_{600} of 0.4 and RNA was extracted using a Machery-Nagel kit, following manufacturer protocol. Following RNA elution, RNA quantity and quality was quantified using Qubit RNA and dsDNA quantification kits. Extracted RNA was used for cDNA synthesis using Thermo Scientific Maxima cDNA synthesis kit. Primers specific to the genes of interest (*gyrA, perR, fetB, VIT, saeR,* and *mtsA*) were designed, with *gyrA* to act as a housekeeping control. RT-qPCR was conducted on a QuantStudio 3 Real-Time PCR machine using the PowerTrack SYBR Green master mix, and fold change of target genes was identified using mean threshold (Cq) values compared to housekeeping control gene *gyrA*. RT-qPCR analysis was conducted using two-way ANOVA with Dunnett's multiple comparison test.

Oxidative Stress Survival and Breakdown

Hydrogen peroxide (H_2O_2) survival was determined according to the following method. Cultures of GBS WT, mutant, and complement strains were grown in polypropylene tubes

overnight in 2 ml of THB and inoculated (1:10) into the same volume of fresh media and grown to mid-log phase at optical densities of 0.4-0.5. Overnight and mid-log cultures were then normalized to 0.4 OD in fresh media and challenged with 1 mM H_2O_2 and incubated aerobically without agitation at 37°C for three hours. Cultures were then serially diluted, plated on THA, and incubated for 18 hours at 37°C. Colony forming units (CFU) were counted, and cell survival was calculated based on comparison between treated and untreated cultures. To measure breakdown of H_2O_2 by GBS, bacterial cultures were normalized as above in simulated vaginal medium (SVF). H_2O_2 was added to bacterial culture, and remaining H_2O_2 was measured using a Thermofisher Pierce™ Quantitative Peroxide Assay Kit every two hours. Bacterial supernatant was collected by centrifuging the bacterial pellet at 10000rfp for 10 minutes and then removing and filter sterilizing supernatant. Analysis of H_2O_2 survival was conducted using Friedmans and Kruskal-Wallis non-parametric tests with Dunns multiple comparisons, while breakdown of H_2O_2 was analyzed using one-way ANOVA.

Iron Assays

The impact of iron chelation across GBS strains was measured using 2,2-bipyridyl to induce chelation. GBS WT and mutant strains were grown overnight polystyrene tubes in 2 ml volumes of THB, normalized and back diluted to an OD_{600} of 0.01 into THB 2,2-bipyridyl at a concentration of 4mM in 96 well plates. OD_{600} over 18 hours was measured using Biotek Epoch plate reader.

Sequence Alignment and Analysis

Gene identification and protein sequences were acquired from the National Center for Biotechnology Information (NCBI). Protein sequence alignments were performed using NCBI BLAST global alignment and COBALT. Sequence alignment maps were created in Jalview

(Waterhouse 2009). Accession numbers for GBS strains used to identify *perR* conservation were NC_007432.1 (A909), AAJS00000000 (H36B), AAJO01000000 (18RS21), AAJR00000000 (COH1), NZ_LS483342.1 (NCTC11930), NZ_CP063198 (CJB111), NZ_AKXO01000026 (GB00112), and NC_004368 (NEM316). Searches for *per* box-like sequences on promoters were carried out using SnapGene, based on PerR binding motifs observed in *B. subtilus* and GAS (Brenot 2005). GAS *per*-box binding sequence (TTANAATNATTNTAA) matches were identified across the GBS genome allowing for one nucleotide mismatch to identify potential PerR binding sites and establish a consensus *per*-box in GBS. Structural models created using Alphafold3 using GBS PerR protein and zinc and iron cofactors (Abramson 2024).

Results

Hydrogen Peroxide Breakdown

Breakdown of hydrogen peroxide by GBS was investigated in the A909 background, using a WT and *perR* deletion strain. Breakdown of sublethal levels of H_2O_2 over three hours in SVF by both sterilized supernatant from GBS bacterial culture and bacterial culture was measured using a Pierce hydrogen peroxide kit. Sterile supernatants from stationary and log phase GBS culture did not show a significant decrease in H_2O_2 compared to an SVF control, though there was a trend of slightly decreased levels (**Figure 1A**). Stationary phase bacterial culture in both WT and mutant A909 strains showed similar levels of H_2O_2 to control media. However, log phase bacterial culture showed a statistically significant decrease in H_2O_2 compared to stationary phase culture and media controls. No difference was observed between WT and mutant strains however (Fig. 1B). This is a clear indication that GBS can break down H_2O_2, though the lack of breakdown in culture cell-free supernatants suggest that this is most likely not primarily through the production of extracellular peroxidases.

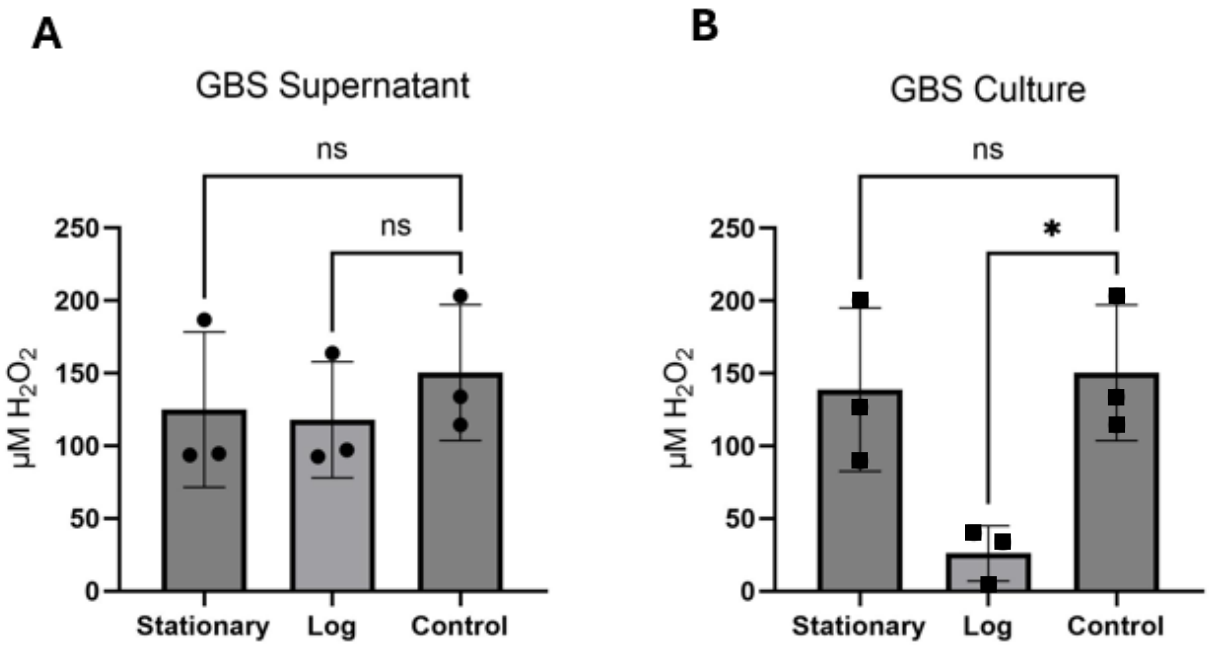

Figure 1: Breakdown of H2O2 by GBS bacterial culture and supernatant (A) GBS A909 WT and perR strains were grown to log and stationary phase in SVF, supernatant was harvested, and 200uM H2O2 was added to supernatant and incubated for 3 hours, and then H2O2 levels were quantified. (B) Strains were grown to log and stationary phase, and then 150uM H2O2 was added and incubated for 3 hours at 37C. H2O2 levels were then quantified and compared to a no-bacteria control. All quantification of peroxide was conducted using Pierce Hydrogen Peroxide Assay Kit. One-way ANOVA where *p<0.05, **p<0.01, ***p<0.001

PerR Structure

To identify similarity of GBS PerR to other known species, a protein sequence alignment was conducted using BLASTp. Percent identity of 71% was identified between the GBS and GAS, indicating a high level of structural similarity (**Figure 2A**). A comparison of PerR sequence similarity across 7 diverse GBS serotypes confirmed the PerR amino acid sequence to be 100% conserved across all strains examined (Kapatai 2017). A multiple sequence alignment was conducted between GAS, GBS and *S. aureus* PerR, as well as *S. aureus* and *B. subtilis* FUR to identify similarity at specific metal binding sites, as previously characterized in GAS (Makthal 2013). Both zinc and the central metal cofactor binding sites are conserved between PerR and Fur across all species. To identify a PerR binding motif in GBS, known *per*-boxes in *B. subtilus* and GAS (TTATAATNATTATAA and TTANAATNATTNTAA respectively), were used to identify potential PerR binding sites in the promoter regions of GBS genes (Figure 2B). Several of these sites were then compared to identify a hypothetical consensus sequence for PerR binding in GBS, currently proposed as TTNTANTNATTNTAA. We then used this proposed *per*-box binding sequence to identify potential genes under *perR* regulation. Several genes of interest were identified as containing a potential *per*-box in their promoter region, including *mtsA, fetB,* and *RS04410* (*VIT*), genes shown or predicted to function in metal import or export. Potential protein structure for GBS PerR was identified using Alphafold3, including predicted zinc and metal cofactor binding sites (Fig. 2C).

Strain Growth and Response to H_2O_2 and Iron Chelation

Deletion mutants lacking *perR* and *perR* complement strains were constructed in two medically relevant GBS strains, CJB111 (serotype V), and A909 (serotype 1a). To establish if deletion of the *perR* gene results in a growth defect in GBS, growth curves were performed using

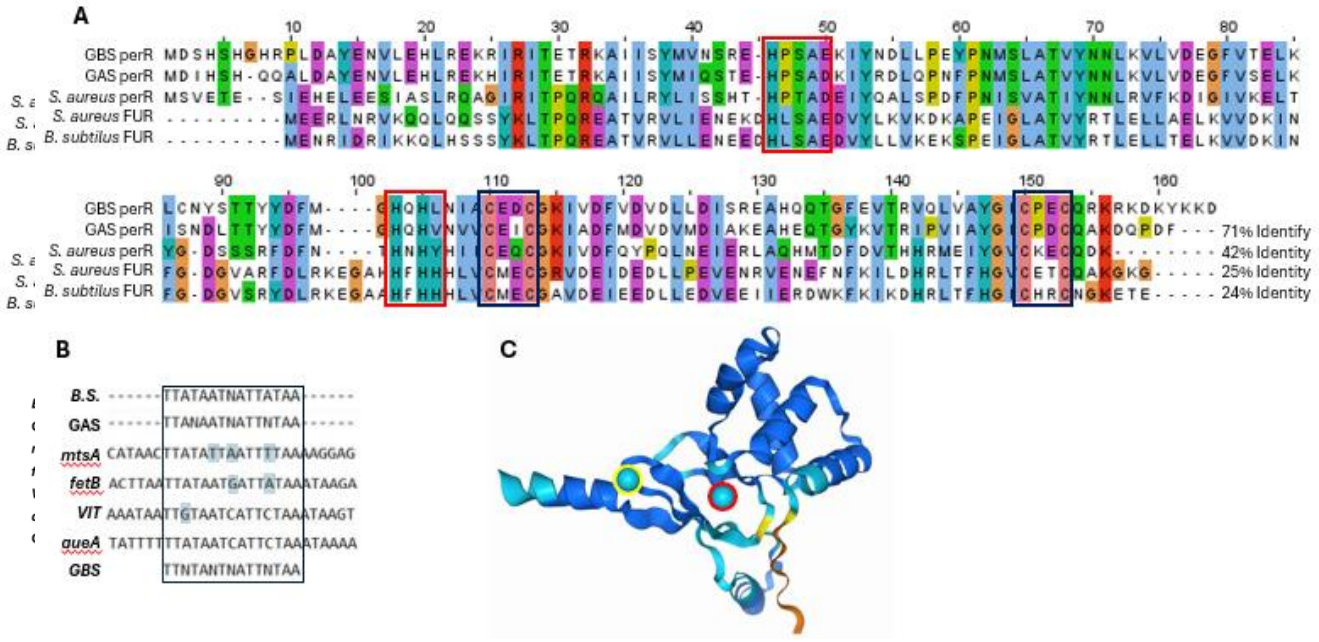

Figure 2: *Streptococcus agalactiae* PerR structure and binding
(A) GBS, GAS, and *S. aureus perR*; and *S. aureus* and *B. subtilus* Fur, aligned to visualize protein homology and color coded using Clustal color schemes in Jalview. Boxes show zinc binding (blue) and central metal binding (red) motifs. Percentage identity calculated using NCBI BLASTp. (B) *Per*-box binding motif for *B. subtilis (B.S)* and GAS was used to identify genes *mtsA, fetB, VIT,* and *queA* which contain similar binding sites, to identify a hypothetical consensus *per*-box motif in GBS. (C) GBS PerR structure predicted by Alphafold3, contains two metal binding sites. One zinc binding C-terminal site (yellow), and one central metal binding site (red).

both rich Todd Hewit Broth (THB) complex media for CJB111 and a more minimal simulated vaginal fluid (SVF) in both strains (**Figure 3, Figure 4**). Absorbance was measured over an 18-hour time course and cultures were plated every two hours to observe changes in CFU. Statistical analysis by two-way ANOVA with Tukeys multiple comparisons revealed no statistically significant difference in growth between WT and mutant strains, though in CJB111 Δ*perR*/pABG5 EV and Δ*perR*/pABG5:*perR* did show a trend towards slightly slower log phases. However, all strains reached the same stationary phase OD_{600}.

As *perR* has been characterized as a repressive regulator of H_2O_2 response in other Gram-positive species, we compared sensitivity of WT, *perR* deletion mutants, and *perR*-expressing complement strains to challenge with H_2O_2. Strains were grown in THB and SVF media with or without H_2O_2 for three hours and plated to determine survival following peroxide stress (**Figure 5**). In THB media, deletion of *perR* in both A909 and CJB111 resulted in increases in survival compared to WT strains, increasing to from 36% to 57% in A909, and from 47% to 65% in CJB111, respectively. However, this increase in survival was only statistically significant in the CJB111 background. While complement strains in both backgrounds showed slightly decreased survival compared to mutant strains, complementation did not fully restore survival to WT levels.

Given the relevance of *perR* as a FUR homolog in GBS, the impact of iron chelation on GBS strains was assessed. Iron chelation was achieved using 2,2-bipyridyl as a chelator of iron in THB media. 2,2-bipyridyl has been well characterized as an iron chelator, though it can also bind some other metals, like copper and nickel, at lower affinities (Romeo 2001). In the CJB111 background, bacterial culture was treated with 2,2-bipyridyl at 4mM concentrations. WT strains showed minimally decreased growth levels, while *perR* deletion strains showed significantly

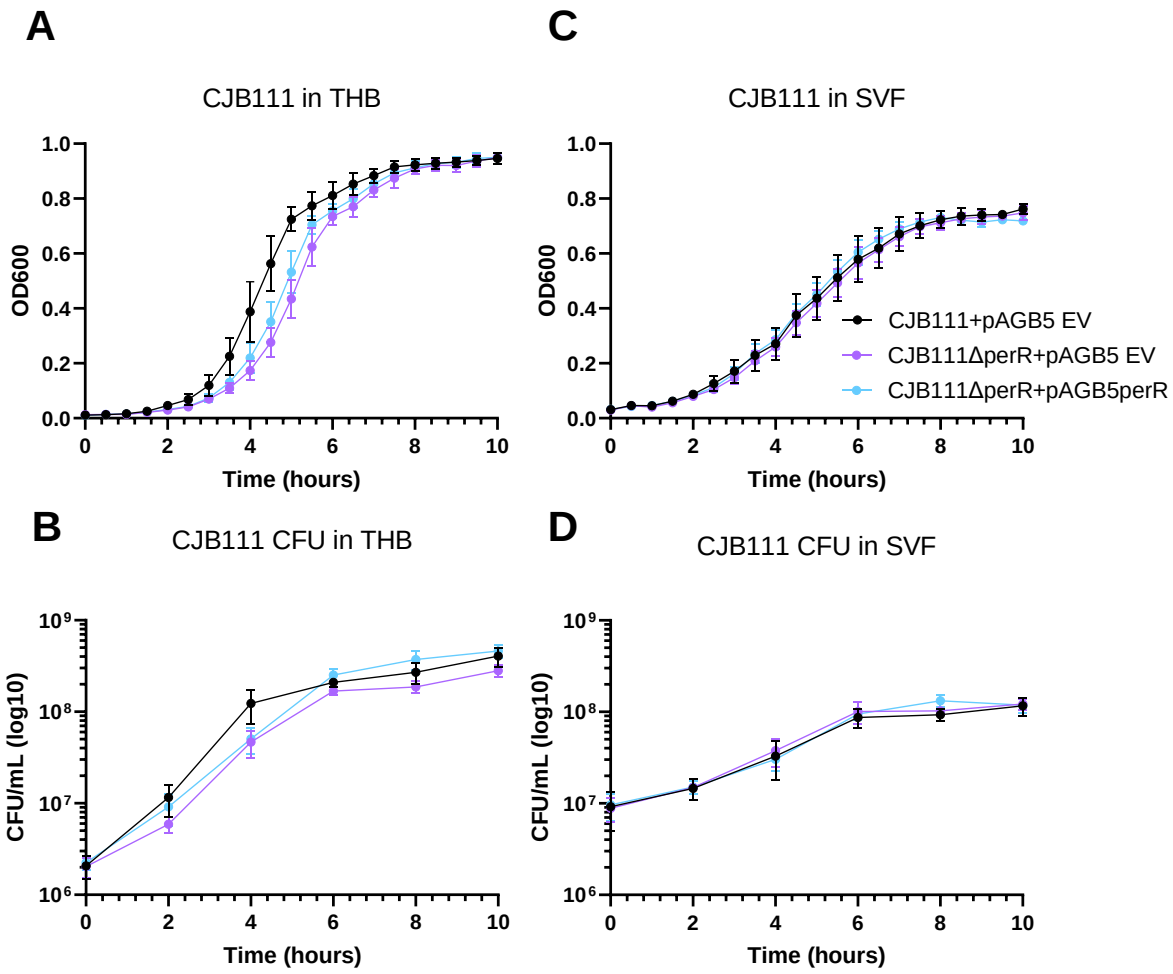

Figure 3: Growth curves and colony counts of GBS CJB111 strains in THB and SVF
GBS CJB111 WT+pABG5 empty vector, *ΔperR*+pABG5 empty vector, and *ΔperR*+pABG5:*perR* strains were grown and OD600 absorbance was measured on a spectrophotometer every 30 minutes and plated on THA media every 2 hours. (A-B)Strains were grown in THB media, starting at 1x10^6 CFU per mL. (C-D) Strains were grown in SVF media, starting at $1x10^7$ CFU per mL. Error bars calculated based on standard error of the mean (SEM).

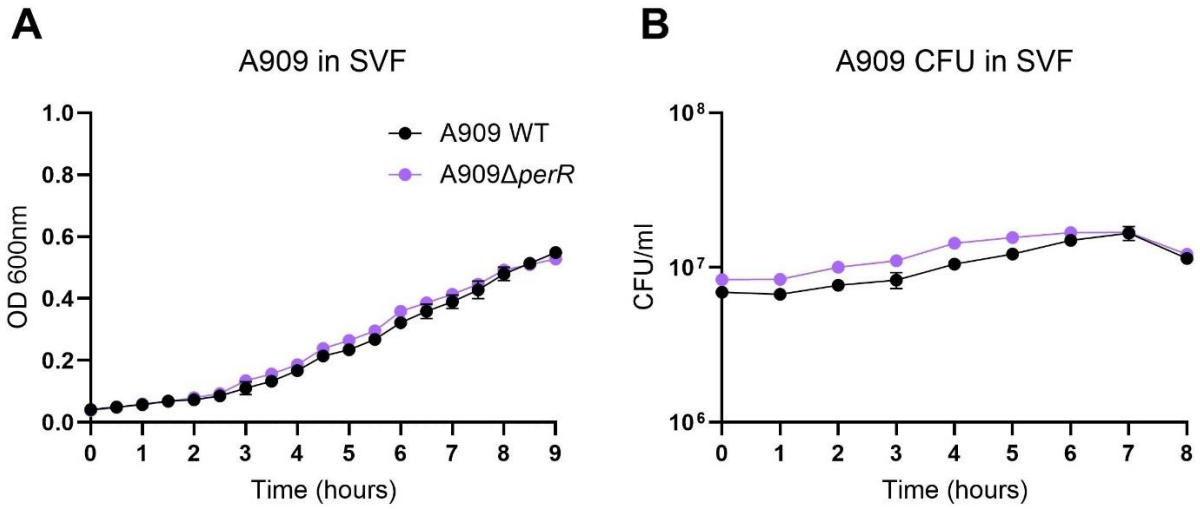

Figure 4: Growth curves and plate counts of GBS A909 strains in SVF
GBS A909 WT and *ΔperR* strains were grown and (A) OD600 absorbance was measured on a spectrophotometer every 30 minutes and (B) plated on THA media every 2 hours. Strains were grown in SVF media, starting at $1x10^7$ CFU per mL. Error bars calculated based on standard error of the mean (SEM). Error bars calculated based on standard error of the mean (SEM).

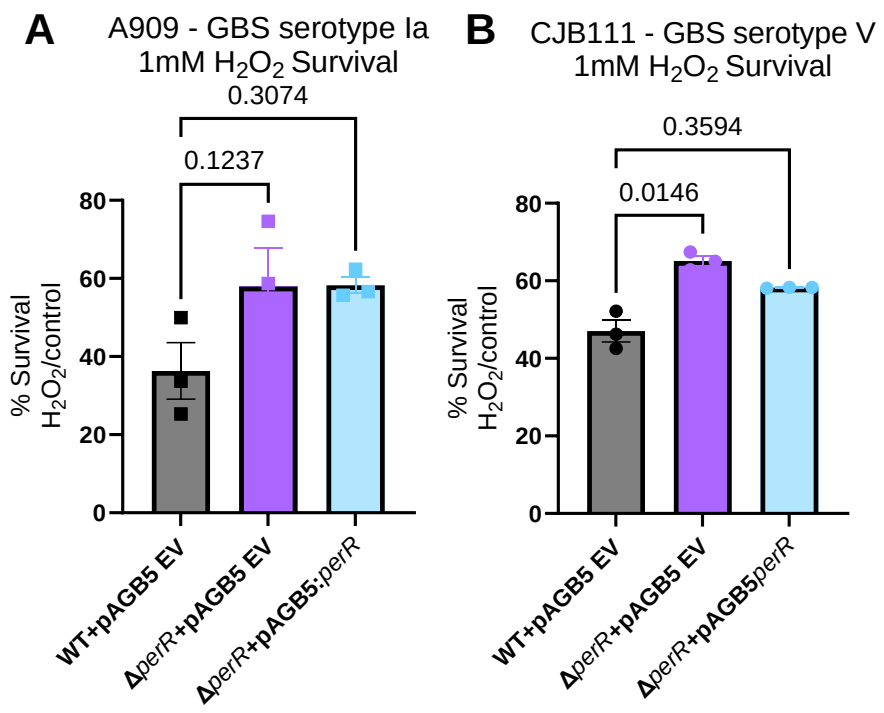

Figure 5: Differential survival of GBS strains with H_2O_2 in complex media
Log phase GBS (A) A909 and (B) CJB111 cultures were exposed to H2O2 stress or left untreated as controls for three hours and then plated on THA media. Survival percentages were calculated by comparing H2O2 treated cultures to untreated controls. Both strains were treated with 1mM H2O2. Data was analyzed using Kruskal-Wallis one way ANOVA.

decreased growth and complement strains showed even greater inhibition than deletion strains (**Figure 6C-D**). However, in the A909 background no difference in strain was observed (Figure 6A-B). This suggests that *perR* plays a role in modulating some portion of iron homeostasis within GBS, as both increasing and decreasing expression of *perR* can impact growth in iron limited conditions. However, this regulatory function seems to vary across GBS serotype.

RNAseq and RT-qPCR

RNAseq was used to identify genes differentially regulated in WT and Δ*perR* background in A909. Analysis of these results identified a number of genes upregulated in the Δ*perR* strain compared to WT. Of these, three genes of note were upregulated in untreated, H_2O_2, and iron chelated conditions, *fetB, saeR,* and a VIT family protein (*VIT*). Interestingly, in the Δ*perR* untreated condition almost every downregulated gene compared to WT mapped to phage elements in the A909 genome (**Table 1**).

We used QRT-PCR to confirm expression levels of *perR* mRNA in CJB111 WT/pABG5 EV, Δ*perR*/pABG5 EV, and Δ*perR*/pABG5:*perR* strains, as well as to identify if expression of specific genes was upregulated in Δ*perR* strains in the CJB111 background, as observed in A909 by RNAseq. Changes in gene expression in response to H_2O_2 and iron chelation using 2,2-bipyridyl were also similarly confirmed. *PerR* showed no meaningful expression in *perR* deletion strains compared to WT, but increased expression compared to WT in the pAGB5:*perR* complement strain (**Figure 7A**). *FetB, saeR, VIT,* and *mtsA* were also investigated in all three CJB111 strains and H_2O_2 and 2,2-biypridyl treatment conditions (Figure B-E). WT, deletion and complement strains showed minimal changes in expression across H_2O_2 and iron chelation treatments, with the exception of *fetB*, which showed 3 fold decrease in expression under H_2O_2 conditions (Figure 7B), and *mtsA* which showed 2.7 fold increase in expression under 2,2-

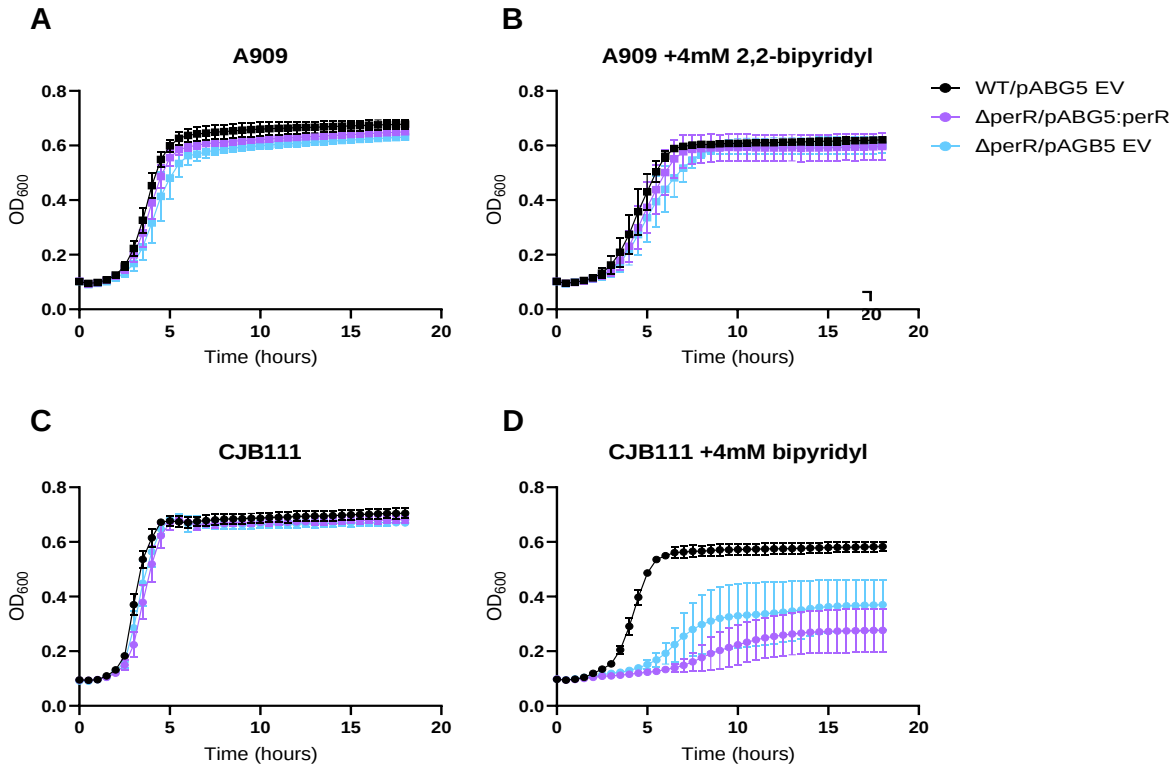

Figure 6: Impact of iron chelation with 2,2-bipyridyl on strain growth
CJB111 and A909 WT+pABG5 empty vector, *ΔperR*+pABG5 empty vector, and *ΔperR*+pABG5:*perR* strains grown with or without 4mM 2,2-bipyridyl chelator. Strains were grown overnight in THB, and then diluted to 0.01 OD in a 96 well plate and measured on a EPOCH Biotech plate reader every 30 minutes. Standard deviation calculated using SEM.

Table 1: RNAseq identified differentially expressed genes Δ*perR* vs WT

Feature ID	Predicted Function	Fold Change
SAK_RS04090	iron export ABC transporter permease subunit FetB	3.64
SAK_RS04615	VIT family protein (vacuolar iron transporter)	3.3
SAK_RS02325	response regulator transcription factor (SaeR)	2.69
SAK_RS00110	tRNA-Leu	2.68
SAK_RS11530	hypothetical protein (phage adjacent)	-2.54
SAK_RS03225	DUF5361 domain-containing protein (phage)	-2.61
SAK_RS03190	hypothetical protein (phage)	-2.86
SAK_RS03215	tail protein (phage)	-2.83

Genes identified in RNAseq with largest fold change increase and decrease in Δ*perR* compared to WT strain of A909.

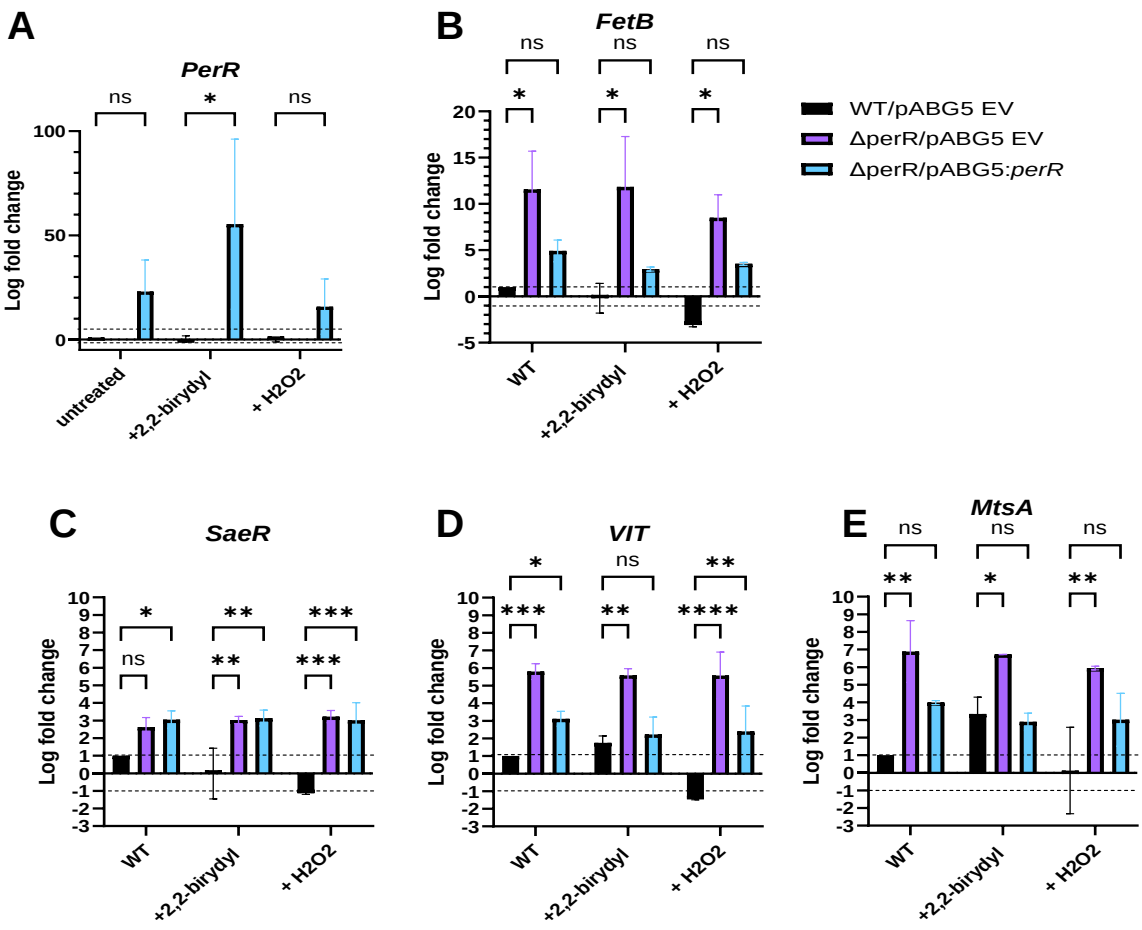

Figure 7: RT-qPCR analysis of differential gene expression in *ΔperR* strains
Differential gene expression of GBS CJB111 WT+pABG5 empty vector, *ΔperR*+pABG5 empty vector, and *ΔperR*+pABG5:*perR* strains, grown in THB, THB + 150µM H_2O_2, or THB+500µM 2,2-bipyridyl. Mean Cq values for (A) *perR*, (B) *fetB*, (C) *SaeR*, (D) *VIT*, and (E) *mtsA* are shown, with fold change compared to untreated WT strain. Dashed lines at +/-one-fold represent WT expression levels. Significance was measured using a two-way ANOVA, where *<0.05, **<0.01, and ***<0.001.

bipyridyl expression (Figure 7E). However, all four genes showed increased expression levels in Δ*perR* strains, with some reduction of expression in the complement background in *fetB, VIT* and *mtsA* (Figure 7 B-E).

Chapter III: Role of *perR* in Colonization and Disease

Introduction

While it is valuable to investigate the growth dynamics and impacts of *perR* in batch culture *in vitro*, it is also important to acknowledge that these environments lack the presence of host pressure or other microbial competitors. To understand the impact of *perR* as a regulator of the peroxide stress response and iron homeostasis in conditions that more closely mimic the host environment, tissue culture and mouse models were used. Immortalized vaginal epithelial (VK2) cells have been a well-established tool for characterizing host/bacterial interactions on a cellular level (Wang 2014, Patras 2018 Given the potential role of *perR* as a direct or indirect regulator of the SaeR/S system, and the regulatory role of SaeR/S in virulence and cellular adhesion, characterizing these interactions in the context of *perR* is important (Coppolino 2024). Murine models of both systemic disease and vaginal colonization have also been used extensively in the study of GBS (Patras 2016, Mendonça 2024). While *Lactobacillus* species are often dominant in human vaginal environments, a humanized murine vaginal model has yet to be developed.

Methods

Murine Models of Vaginal Colonization and Systemic Infection:

All animal experiments conducted were approved by the Institutional Animal Care and Use Committee at the University of Tennessee, Knoxville. Vaginal colonization was performed as described previously (Patras 2016). 8-week-old female ICR (Envigo/Inotiv) and C57BL/6 (Jackson Labs unless noted) were synchronized day -1 using 17β-estradiol administered by intraperitoneal injection at a concentration of 0.5 mg/100μL. Bacterial cultures were grown overnight, diluted (1:10) into fresh culture media the following day, and grown to ~0.4 OD_{600}. Cultures were normalized to 0.4 OD_{600} in PBS, concentrated 10-fold, and mice were colonized

intravaginally with $1x10^7$ CFU/10µL GBS. Following colonization, mice were vaginally swabbed daily (ICR) or every other day (C57BL/6) and swabs were plated on Strep B CHROMagar to monitor bacterial burden. Mice were euthanized day 6 (ICR) or day 12 (C57BL/6), and vaginal, cervical, and uterine tissues were harvested and plated for CFU counts. Systemic challenges were inoculated retro-orbitally, as described previously (da Conceição Mendonça 2024). Female 8-week-old ICR (Envigo/Inotiv) and C57BL/6 (Jackson) mice were infected with $1x10^7$ CFU CJB111 or $2\text{-}3x10^8$ CFU A909 in a 100µl volume. GBS strains were prepared in the same way as in the murine vaginal colonization model, with the only change being that following normalization to 0.4 OD_{600} in PBS of log phase cultures, strains were then used for infection in CJB111 or concentrated 20-fold and then used for infection in A909. All mice were monitored for the onset of clinical symptoms of systemic disease based on a symptom score checklist accounting for changes in grooming, movement/gait, righting reflex, feeding/drinking, breathing effort, and onset of neurological symptoms. When animals reached a moribund status (score of >12 on mouse grimace scale) or the 48h experimental timepoint, brain, heart, lung and blood were harvested. Tissues were homogenized in 500µl PBS and all samples were serially diluted and plated on Todd Hewitt Agar to enumerate bacterial burden. Organs were still collected and plated for animals euthanized before the 48 hour timepoint, so bacterial burden at time of death could still be accounted for. For the neutrophil depletion model of systemic disease, anti-mouse Ly6G (BioXCell) antibodies were used for neutrophil depletion, with the rat IgG2a anti-trinitrophenol isotype control (BioXCell). Mice were injected I.P. with 200ug antibody in 100ul PBS day -1 of infection. Following antibody treatment, experiment was performed as described previously for the systemic disease model. For vaginal colonization and systemic disease models n=10, though n=8 was used in the neutrophil depletion experiment.

Data was analyzed using Mann-Whitney nonparametric tests for tissue analysis with the exception of neutrophil depletion mice in which a two-way ANOVA was used. Using uncorrected fisher's LSD for multiple comparisons. Swabs were analyzed using two-way ANOVA with Sidak's multiple comparisons test, and survival curves using log-rank mantel-cox test.

Vaginal Cell Assays

Vaginal epithelial cell adherence assays were performed as previously described (Jiang 2012). Vaginal epithelial VK2 cells were seeded in 24 well plates at $1.75x10^5$ cells and growth to a monolayer. Bacteria were grown to mid-log phase (OD 0.4), or approximately $1x10^8$ CFU/mL, and added to epithelial cells at a MOI of 10:1 and incubated at 37C for 30 minutes. To assess adherence cells were then washed 5 times with PBS, detached with 0.25% trypsin, and lysed with 0.025% Triton X-100. Solution was then diluted and plated for CFU counts. Data are represented as a percentage of attached bacteria compared to input. Experiment was analyzed using two-way ANOVA.

Growth in Human Blood

Growth assays in human blood were performed by collecting 10ml fresh blood using a butterfly needle from a donor in an EDTA treated tube to prevent coagulation under UTK IRB-14-06476-XP. Bacterial strains were grown overnight in THB and then inoculated 1:10 into fresh THB culture and grown to log phase at OD ~0.4, and normalized to OD_{600} 0.4 in PBS ($1x10^8$ CFU/ml). Bacteria were then added to blood at a concentration of $1x10^7$ CFU/ml, and incubated rotating at 37 °C for 6 hours, plated at time 0 and every two hours for 6 hours on THB to establish CFU counts.

Results

Murine Model of Vaginal Colonization

To identify the impact of the *perR* gene on the ability of GBS to colonize and persist in the vaginal tract, a murine vaginal model of GBS colonization was used. WT and *perR* mutant strains in both the A909 and CJB111 GBS backgrounds were used, and GBS vaginal persistence was measured as well as GBS burden in vaginal, cervical, and uterine tissues. ICR outbred mice were used to for one colonization experiment with CJB111 to match the same strain and mouse line used in the *Krmit* tnseq library experiment (Burcham 2022), and C57BL/6 mice were used for all other experiments as they are less likely to clear GBS colonization. In the A909 strain, colonization in C57BL/6 mice was performed two times to confirm phenotype. However, by accident mice were ordered from two different vendors. In the first experiment, using 9-week old C57BL/6N Envigo/Inotiv mice, there was no significant difference detected in vaginal colonization between WT and the *perR* mutant strain, though a significant increased recovery of the *perR* mutant was observed specifically in uterine tissue of C57BL/6 animals (**Figure 8**). However, in the second experiment with A909 and C57BL/6 mice sourced from Jackson laboratory, no difference in uterine bacterial burden was observed (**Figure 9**). In the CJB111 background, there were no significant difference observed between strains in vaginal swabs or reproductive tissues harvested from C57BL/6 animals (**Figure 10**), while in CD-1 mice the *perR* deletion strain showed a trend of decreased vaginal persistence, and significantly decreased bacterial burden in vaginal, cervical and uterine tissues following tissue harvest (**Figure 11**). This data suggests that *perR* is not a driving regulatory factor in vaginal colonization and persistence but may still regulate some factors that contribute to GBS colonization. However, differences across animal background make a conclusive answer hard to identify. Data was

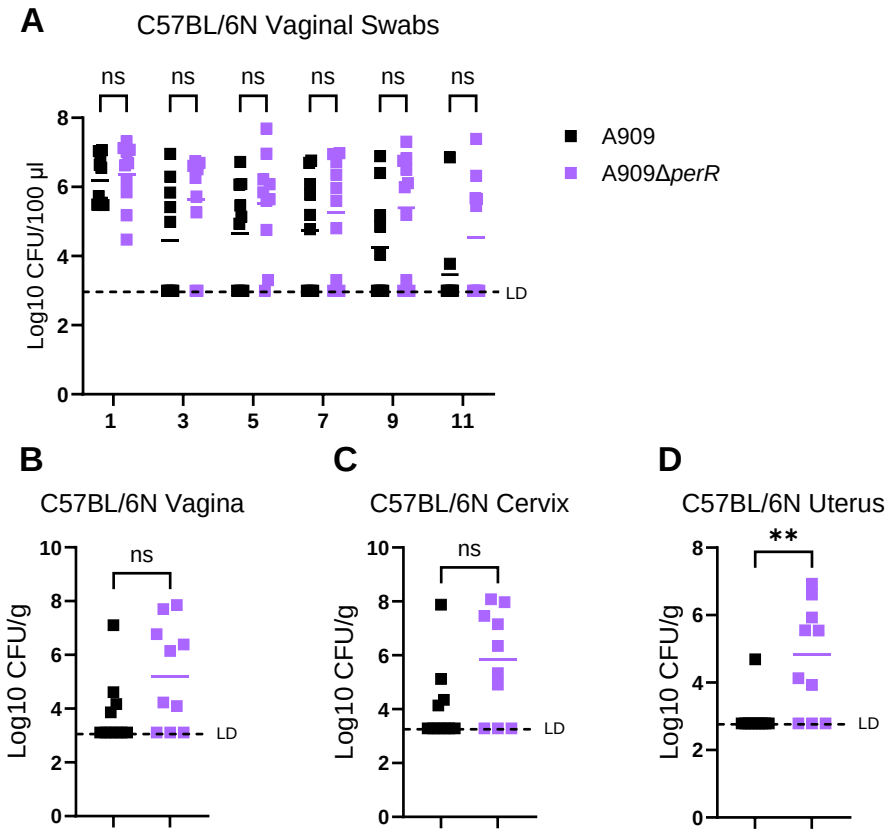

Figure 8: A909 murine vaginal colonization model in 5-week C57BL/6N
CD57BL/6N 9-week-old mice sourced from Inotiv were colonized with $1x10^7$ CFU A909 WT and Δ*perR* strains of GBS. (A) Mice were vaginally swabbed every other day post colonization, and CFUs calculated by plating on THA media. (B-D) Vaginal, cervical and uterine tissues were then harvested and plated to identify bacterial burden in the reproductive tract. Symbols represent individual animals (WT n=10, Δ*perR* n=10). Swabs were analyzed using a two-way ANOVA, and tissues using either a Mann-Whitney or Kolmogorov-Smirnov non-parametric test.

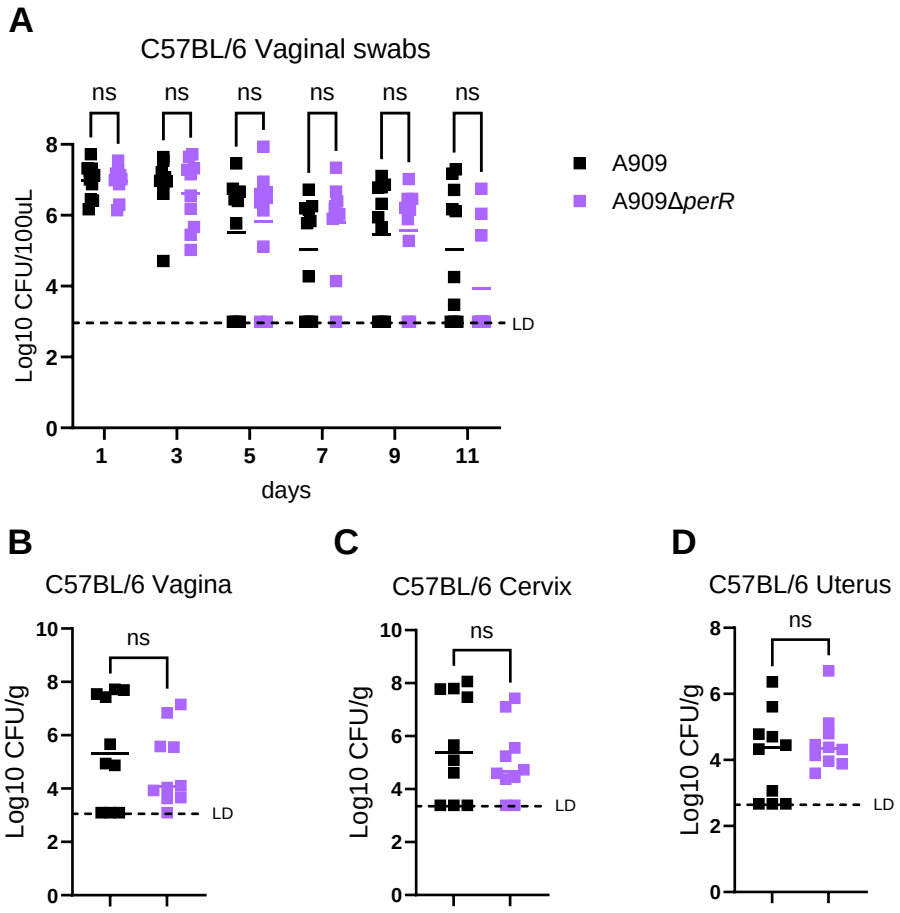

Figure 9: A909 murine vaginal colonization model in 9-week old C57BL/6J
CD57BL/6J 5-week old mice sourced from Jackson laboratory were colonized with $1x10^7$ CFU A909 WT and Δ*perR* strains of GBS. (A) Mice were vaginally swabbed every other day post colonization, and CFUs calculated by plating on THA media. (B-D) Vaginal, cervical and uterine tissues were then harvested and plated to identify bacterial burden in the reproductive tract. Symbols represent individual animals (WT n=10, Δ*perR* n=10). Swabs were analyzed using a two-way ANOVA, and tissues using either a Mann-Whitney or Kolmogorov-Smirnov non-parametric test.

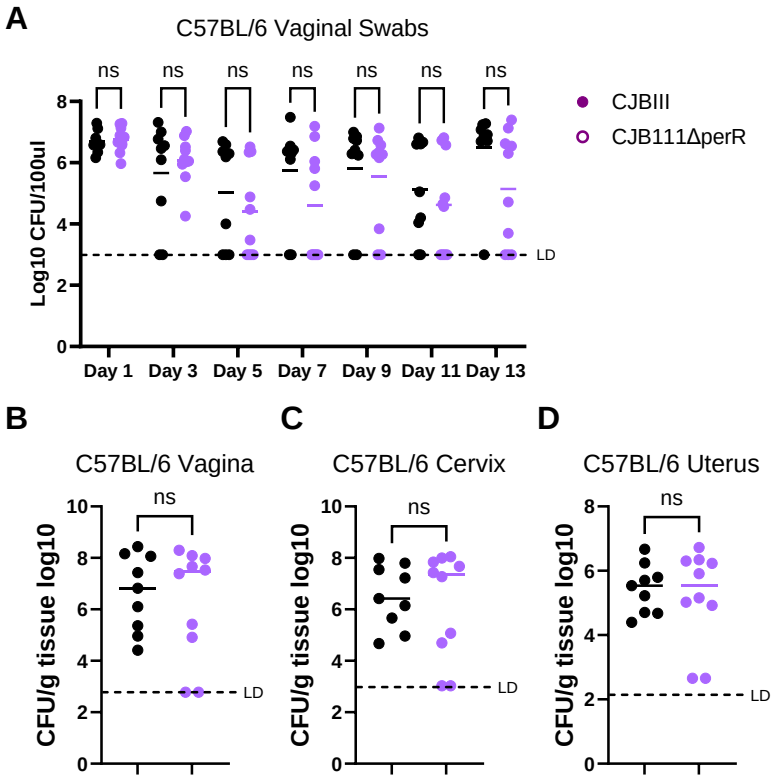

Figure 10: CJB111 murine vaginal colonization model in C57BL/6
CD57BL/6 6-week old mice sourced from Jackson Laboratory were colonized with $1x10^7$ CFU CJB111 WT and Δ*perR* strains of GBS. (A) Mice were vaginally swabbed every other day post colonization, and CFUs calculated by plating on THA media. (B-D) Vaginal, cervical and uterine tissues were then harvested and plated to identify bacterial burden in the reproductive tract. Symbols represent individual animals (WT n=9, Δ*perR* n=10). Swabs were analyzed using a two-way ANOVA, and tissues using either a Mann-Whitney or Kolmogorov-Smirnov non-parametric test.

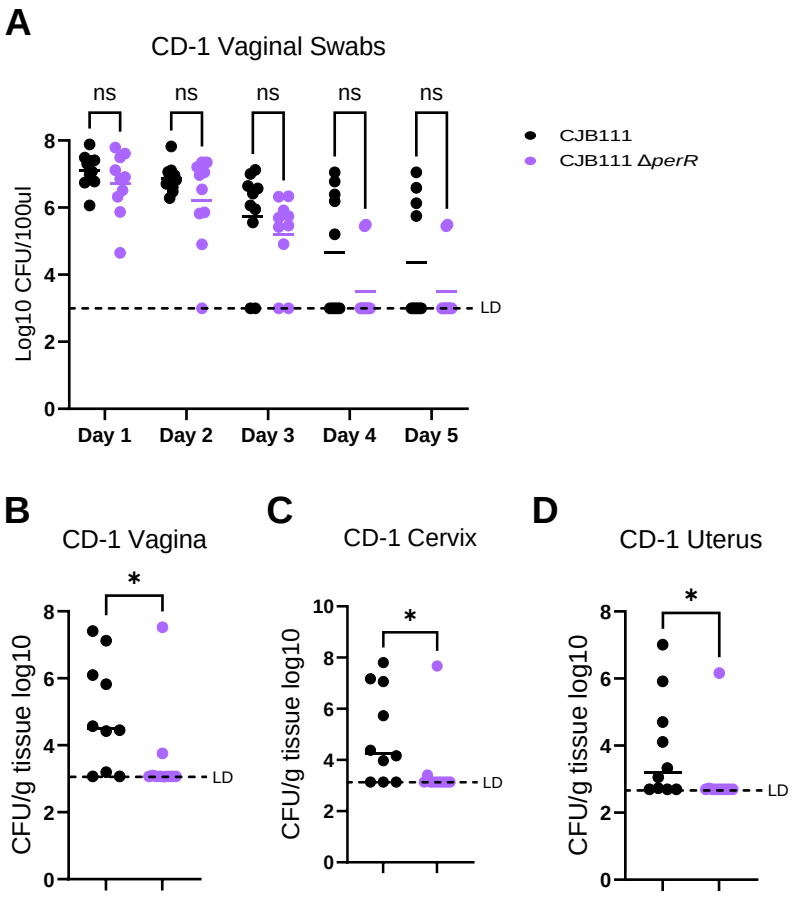

Figure 11: CJB111 murine vaginal colonization model in CD-1 mice
CD-1 6-week old mice sourced from Jackson Laboratory were colonized with $1x10^7$ CFU CJB111 WT and Δ*perR* strains of GBS. (A) Mice were vaginally swabbed every other day post colonization, and CFUs calculated by plating on THA media. (B-D) Vaginal, cervical and uterine tissues were then harvested and plated to identify bacterial burden in the reproductive tract. Symbols represent individual animals (WT n=9, Δ*perR* n=10). Swabs were analyzed using a two-way ANOVA, and tissues using either a Mann-Whitney or Kolmogorov-Smirnov non-parametric test.

analyzed using Mann-Whitney and Kolmogorov-Smirnov nonparametric tests, and two-way ANOVAs with Sidak multiple comparisons.

Vaginal Cell Assays

To understand the impact of *perR* on interactions with host vaginal cells, GBS A909 and CJB111 WT and *perR* deletion strains were tested for adhesion to vaginal epithelial cells *in vitro*. Strains in the A909 GBS background showed increased adherence to host cells compared to CJB111 strains. In the A909 background *perR* mutants did not show significant changes in adherence compared to WT or complement strains **(Figure 12A**). CJB111 strains did show a trend of increased adherence in the *perR* mutant strain over WT and complement strains, though this was not statistically significant as determined by one-way ANOVA using Dunnett's multiple comparison test (Figure 12B). These data indicate that *perR* does not play a significant role in regulation of adherence or other factors that contribute to GBS host cell attachment, and that differences observed between WT and *perR* mutant strains in animal models are most likely not caused by differences in cell adherence.

Murine Model of Systemic Disease

Given the relevance of GBS in the broader context of systemic disease, the importance of *perR* was investigated using a murine model. Similarly to the vaginal model C57BL/6 mice were used to identify the impact of *perR* on virulence in both the A909 and CJB111 backgrounds. Health scores of animals were cataloged over the course of the experiment, as was animal survival, with all remaining animals euthanized after 48 hours. When infected with A909 strains, C57BL/6 WT infected mice showed 44% survival, compared to 80% among those infected with the *perR* mutant (**Figure 13A**). Similarly, increased health scores, meaning increased visible progression of disease, was observed in the WT infected mice (Figure 13B). While no significant

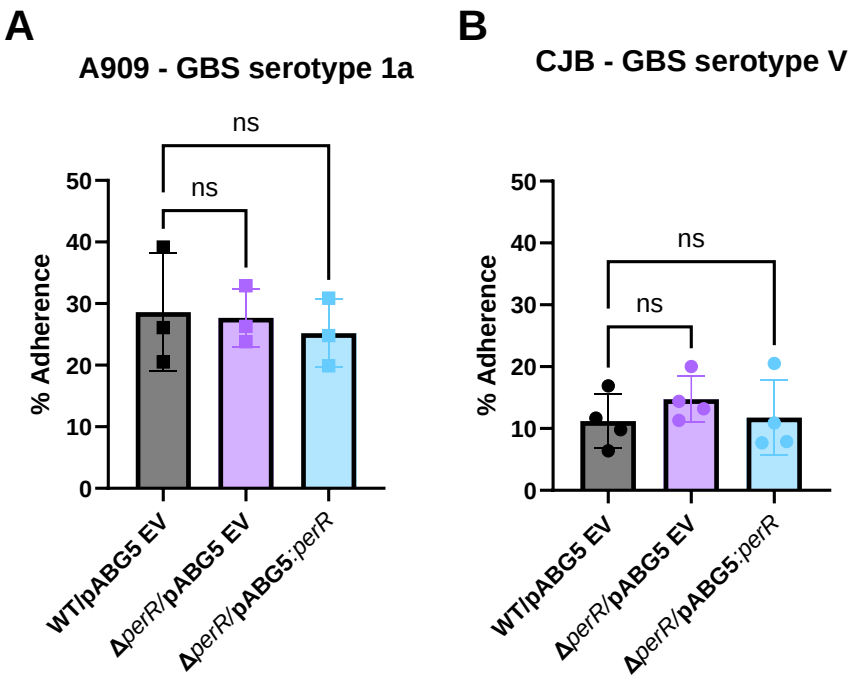

Figure 12: GBS A909 and CJB111 adhesion to vaginal epithelial cells
Adherence of GBS A909 and CJB111 WT+pABG5 EV, *ΔperR*+pABG5 EV, and *ΔperR*+pABG5:*perR* strains were tested by incubation with VK2 cells for 30 minutes at an MOI of 2:1 bacterial to eukaryotic cell. % adherence was calculated by comparing total bacterial inoculation against plated CFU counts following incubation. Significance was measured using a one-way ANOVA.

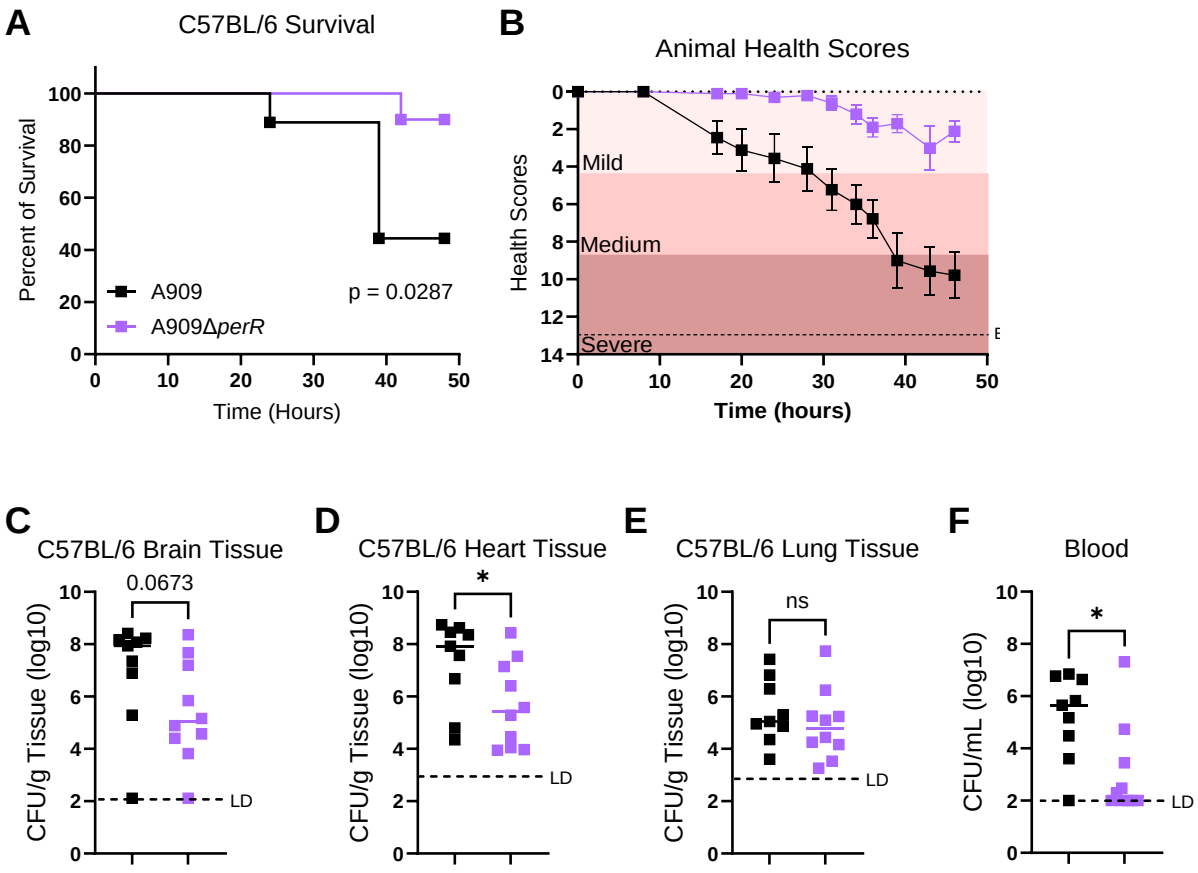

Figure 13: A909 murine model of systemic disease in C57BL/6
6-week old C57BL/6 mice sourced from Jackson Laboratory were infected retro-orbitally with 2-3x10^8 CFU A909 WT or Δ*perR* strains of GBS. Animals were monitored for (A) survival and (B) health scores over a 48-hour period. Health scores were calculated using the mouse grimace scale, and a score of higher than 12 resulted in euthanasia. At experiment end, (C-F) brain, heart and lung tissues, as well as blood was harvested and plated on THA media to enumerate bacterial burden. Statistics were calculated using Mann-Whitney non-parametric tests, where *<0.05. N=10 for each experimental group.

difference in bacterial burden was noted in the lungs, the mutant showed significantly decreased CFU counts in heart tissue and blood, as well as lower (P=0.067) levels in the brain (Figure 13C-F).

CJB111 *perR* mutant infected mice showed 100% survival over 48 hours, compared to 0% in C57BL/6 mice challenged with WT GBS (**Figure 14A**). A clear difference in health scores was also observed, though due to rapid mortality observation was limited in the WT group (Figure 14B). The CJB111 *perR* mutant strain also showed significantly decreased bacteria burden in brain, heart and lung tissue, as well as blood, following experiment end and tissue harvest (Figure 14 C-F).

Infection with CJB111 strains was also conducted in a neutrophil depletion model of C57BL/6 mice, using intraperitoneal injections of anti-Ly6G antibody for antibody depletion and IgG as a monoclonal control. In this model, both WT and *perR* deletion strains showed increased severity of disease in neutrophil depleted mice compared to non-depleted controls. This was observed by increased mortality in WT infected depleted mice (**Figure 15A**), and increased health scores of *perR* deletion infected depleted mice (Figure 15B). WT infected mice also showed significantly higher bacterial burden in brain and lung tissue as well as blood, in both depleted and non-depleted mice (Figure 14 C-E).

Growth in Blood

To determine if the decreased virulence of the *perR* deletion mutants was due to a bottleneck for survival in the blood, GBS survival was measured in human blood. Human blood was collected from donors in EDTA treated tubes to prevent coagulation. Log phase WT, *perR* mutant, and complement strains in both A909 and CJB111 backgrounds were added to whole blood and measured via CFU plate counts every two hours for 6 hours (**Figure 16**). All strains

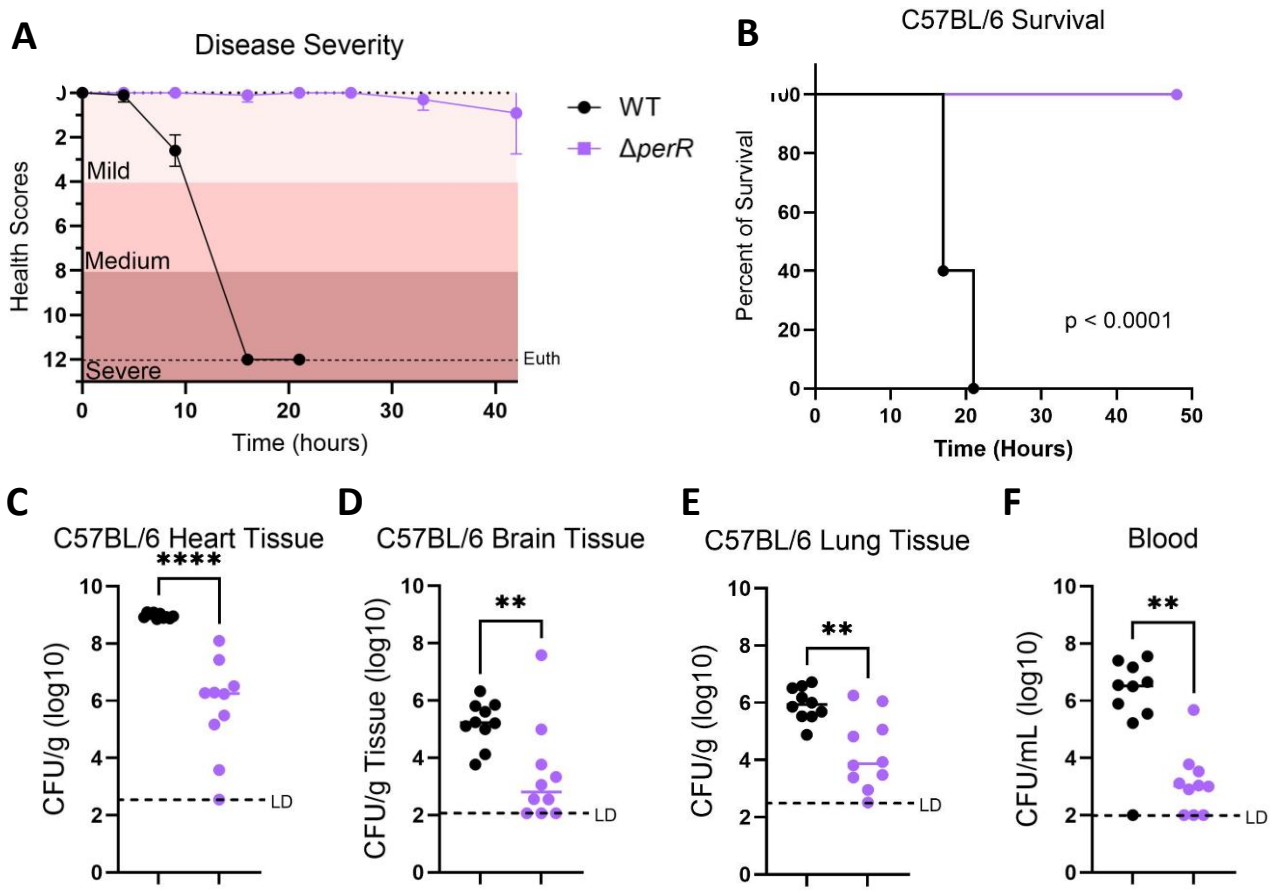

Figure 14: CJB111 murine mode of systemic disease in C57BL/6
6-week old C57BL/6 mice sourced from Jackson Laboratory were infected retro-orbitally with $1x10^7$ CFU CJB111 WT or Δ*perR* strains of GBS. Animals were monitored for (A) survival and (B) health scores over a 48-hour period. Health scores were calculated using the mouse grimace scale, and a score of higher than 12 resulted in euthanasia. At experiment end, (C-F) brain, heart and lung tissues, as well as blood was harvested and plated on THA media to enumerate bacterial burden. Statistics were calculated using Mann-Whitney non-parametric tests, where **<0.01, ****<0.0001. N=10 for each experimental group.

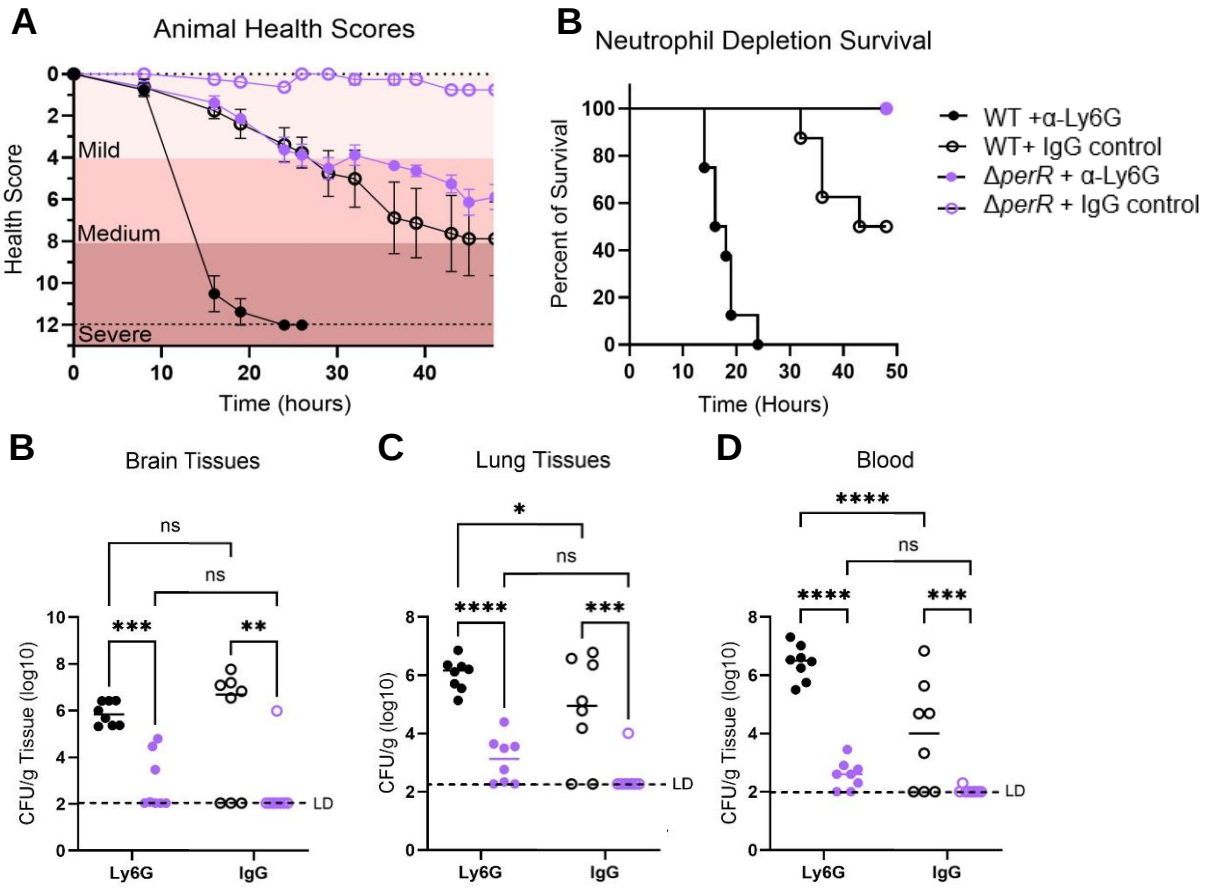

Figure 15: CJB111 murine model of systemic disease in neutrophil depleted C57BL/6
C57BL/6 mice were treated on day -1 of infection with a dose of 200ug A8 monoclonal antibodies (anti-mouse Ly6G) administered I.P. for the Ly6G neutrophil depletion group, and with 2A3 monoclonal antibodies (rat IgG2a isotype control, anti-trinitrophenol) for the IgG control group. Mice were then infected retro-orbitally with $1x10^7$ CFU CJB111 WT or Δ*perR* strains of GBS. Animals were monitored for (A) survival and (B) health scores over a 48-hour period. Health scores were calculated using the mouse grimace scale, and a score of higher than 12 resulted in euthanasia. Neutrophil depleted mice shown in purple, control mice in blue. At experiment end, (C-E) brain and lung tissues, as well as blood were harvested and plated on THA media to enumerate bacterial burden. Statistics were calculated using two-way ANOVA for tissues and blood, where *<0.05, **<0.01, ***<0.001, and****<0.0001. A log-rank Mantel-Cox test was used for animal survival. N=8 for each experimental group.

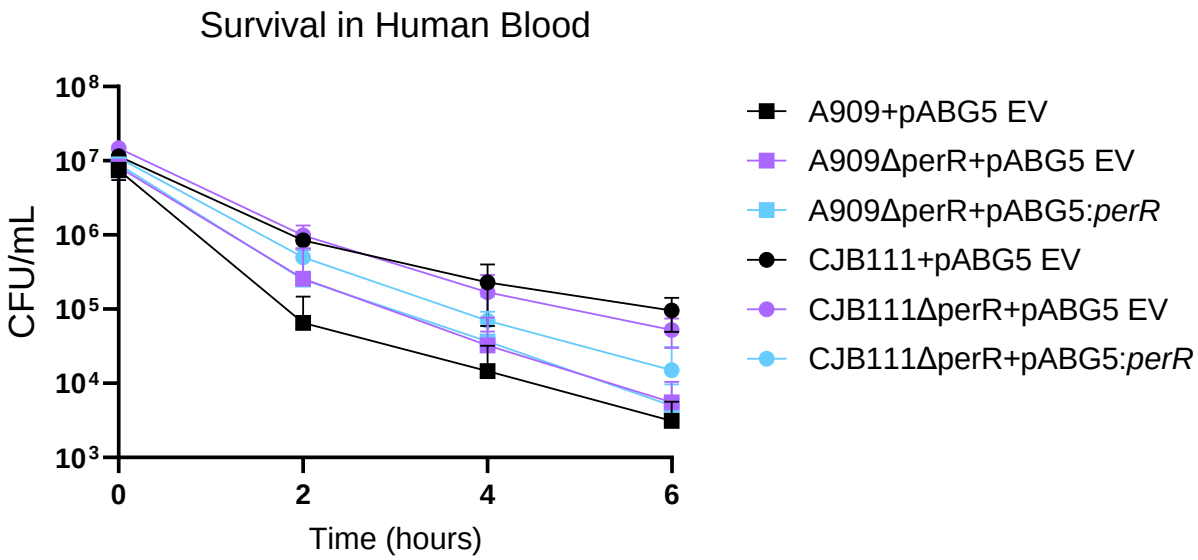

Figure 16: Survival of A909 and CJB111 strains in human blood
Human blood was collected and inoculated with $1x10^7$ A909 and CJB111 WT+pABG5 EV, *ΔperR*+pABG5 EV, and *ΔperR*+pABG5:*perR* GBS strains. Blood was incubated rotating at 37°C for six hours, plating every two hours on THA plates to establish CFU counts. The limit of detection for this experiment was $1x10^3$ CFU. Analysis was conducted using area under the curve and then a two-way ANOVA, and no statistically significant difference was observed between WT, *ΔperR* and complement strains in either GBS background.

showed rapid death in blood over 6 hours, with CJB111 surviving better than A909, but no significant difference was observed between WT, mutant and complement strains. Growth in blood was conducted at three separate intervals using two donors, and analyzed using a two-way ANOVA with Tukeys multiple comparison test. This data suggests that inhibitory factors in human blood, whether immune cells or nutrient availability, make it difficult for GBS to persist regardless of deletion of *perR*.

Chapter IV: Discussion

Colonization by GBS is prevalent across all populations, and because of its flexibility as an opportunistic pathogen and implications for maternal-fetal health it is of global clinical significance. However, different governments and medical societies hold differing views on the best methods of screening and when to apply treatment for GBS in pregnant individuals (Morgan 2025). This is in part because much is still unknown about why GBS causes disease in some cases but not in others, and how different host factors might facilitate or prevent GBS pathogenicity. It is important to continue to characterize what contribute to GBS colonization and persistence in the vaginal environment, and what factors contribute to disease in pregnancy, in a neonate, or in other at-risk populations.

One method we have previously utilized to address some of these questions is a murine model of vaginal colonization using a GBS transposon mutant library (Burcham 2022). As the gene *perR* was both identified by this library colonization as underrepresented in sequencing following colonization and has been identified as a regulator of H_2O_2 stress in other organisms, it was selected as the target for this study. We hypothesize that within GBS, *perR* functions as a regulator of the bacteria's response to ROS stress as well as contributing to metal homeostasis, in particular in regard to iron as the sole Fur homolog of GBS.

We have demonstrated in this study that GBS is able to facilitate the breakdown of H_2O_2, as well as tolerate it at relatively high levels despite the lack of catalase. We have also shown that *perR* does act as a regulator of H_2O_2 stress in GBS, as *perR* deletion strains in two different GBS serotypes show either a significant increase or a trend of increased survival to H_2O_2 stress in a *perR* deletion background compared to WT strains (Fig. 4). This finding, along with the literature of *perR* in other Gram-positive bacteria like *B. subtilus* and *S. aureus* supports the role

of *perR* as a regulatory repressor in GBS, repressing gene transcription and de-repression based on environmental cues (Bernot 2005, Giedroc 2009). Based on protein alignment and protein structural predictions we hypothesize that PerR binds zinc at a structural site and then minds an additional regulatory metal at a central binding site, most likely iron or manganese based on its similarities in structure to GAS PerR.

To begin to characterize the regulon of *perR* in GBS, a twofold approach was taken. RNAseq was conducted on the A909 WT and Δ*perR* strains, grown in SVF and then exposed to iron chelation and ROS stress, utilizing 2,2-bipyridyl and H_2O_2 respectively. Genes that were differentially regulated in all conditions in the Δ*perR* strain compared to the WT show evidence of potential direct regulation (if gene expression is increased in Δ*perR*) or indirect regulation (if gene expression is decreased). This was combined identification of a putative consensus *per*-box motif that is targeted by PerR for binding and repression, based identified *per*-box sites in *B. subtilus* and *S. aureus* as well as comparison of the promoter regions of genes identified by RNAseq as potentially within the regulon of *perR.* This combined analysis was used to identify genes highly likely to be directly regulated by PerR DNA binding. Given that RNAseq was conducted in the A909 background with only WT and Δ*perR* strains, QRT-PCR was conducted in the CJB111 background on WT+pABG5 EV, *ΔperR*+pABG5 EV, and *ΔperR*+pABG5:*perR* strains to confirm similar results in CJB111, as well as to test if complementation using a *perR* expression vector would restore WT gene repression. We showed that in *fetB, VIT,* and *mtsA,* expression increased in the *ΔperR*+pABG5 EV strain, and was reduced, though not to WT levels, in the and *ΔperR*+pABG5:*perR* strain, supporting that these genes are regulated by *perR*. *SaeR* also saw increased expression in *ΔperR*+pABG5 EV, but expression was not decreased in the complement strain. This may indicate a more complex regulatory network for *SaeR*, or that

multiple regulatory factors are at play. Additionally, though search with the putative consensus *per*-box motif does not identify a *per*-box within the promoter region of *saeR,* there is a binding site that shows similar characteristics, like the inverted repeat associated with Fur family binding. This may suggest that additional genomic analysis is needed for identification of a more accurate *per*-box binding sequence for GBS, that PerR may bind more promiscuously than predicted, or that it may impact *saeR* expression in an indirect way.

While direct regulation of genes involved in several genes identified in the H_2O_2 response of GBS (GOH 2024), like *ahpC, tpx,* and *npx,* was not observed either by sequencing or through *per*-box prediction¸ there is a well-established link between metal homeostasis and ROS resistance in bacteria. An *mtsA* mutant of GBS has been shown to have increased sensitivity to ROS, and in *Streptococcus suis mtsA* and manganese import increases the ability of the bacteria to resist ROS (Burcham 2022, Peng 2021). *FetB* also contributes to ROS resistance in *Escherichia coli,* though this iron export system is uncharacterized in *Streptococcus* species (Nicolaou 2013). This indicates that increased resistance to H_2O_2 survival observed in GBS may be due to its role as a regulator of metal homeostasis, rather than direct regulation of peroxide response genes.

This study also demonstrated a strain dependent difference in resistance to iron starvation between A909 and CJB111 strains. While growth under iron chelation using 2,2-bipyridyl of A909 strains showed no difference between WT, mutant and complement strain, growth in CJB111 mutant and complement strain was significantly decreased compared to the WT strain. Rather than restoring survival, the complement strain showed a trend towards further inhibition. This could be due to the limitations of a plasmid-based complementation system, such as differences between WT and complement expression of the gene of interest, or variation in

plasmid copy number. QRT-PCR on CJB111 strains identified that the *⊿perR*+pABG5:*perR* strain shows increased expression of *perR* compared to the WT+pABG5 EV strain. Variation across strain, as well as challenges in effectively testing iron toxicity, complicate a clear iron-based phenotype driven by *perR* deletion. However, in both CJB111 and A909 backgrounds *perR* seems to play a role in regulating iron homeostasis based on its regulation of different characterized and putative iron importers and exporters. While a *perR* deletion CJB111 exhibits a greater sensitivity to iron chelation phenotype though the same strain in A909 does not, differences in GBS serotype or varied sensitivity to changes in metal homeostasis may be responsible for this discrepancy

In this study, we have made the first steps towards characterizing the impact and breadth of the *perR* regulon within GBS, and its impact on the response to H_2O_2 stress and metal homeostasis. From this work we propose a hypothetical physiological model of *perR* regulation and its impact on different metal homeostasis systems and H_2O_2 stress, though the mechanism of H_2O_2 regulation is yet to be isolated (**Figure 17**). We have also begun to characterize its role in interactions with the host, both in the context of vaginal colonization and systemic disease. When tested for adherence to vaginal epithelial cells, no significant difference between strains in either the A909 or CJB111 background was identified. This was a slightly surprising result, as we have shown *saeR* shows increased expression in Δ*perR* strains, and it is a positive regulator of several factors involved in cellular adhesion and invasion (Cook 2018).

While *perR* was significantly underrepresented in vaginal tissue in the *Krmit* tnseq colonization, we have observed varied results using murine colonization models to study the impact of *perR* on vaginal colonization and persistence. It is important to note that all animal work was conducted using WT and Δ*perR* strains without the pABG5 plasmid vector or *perR*

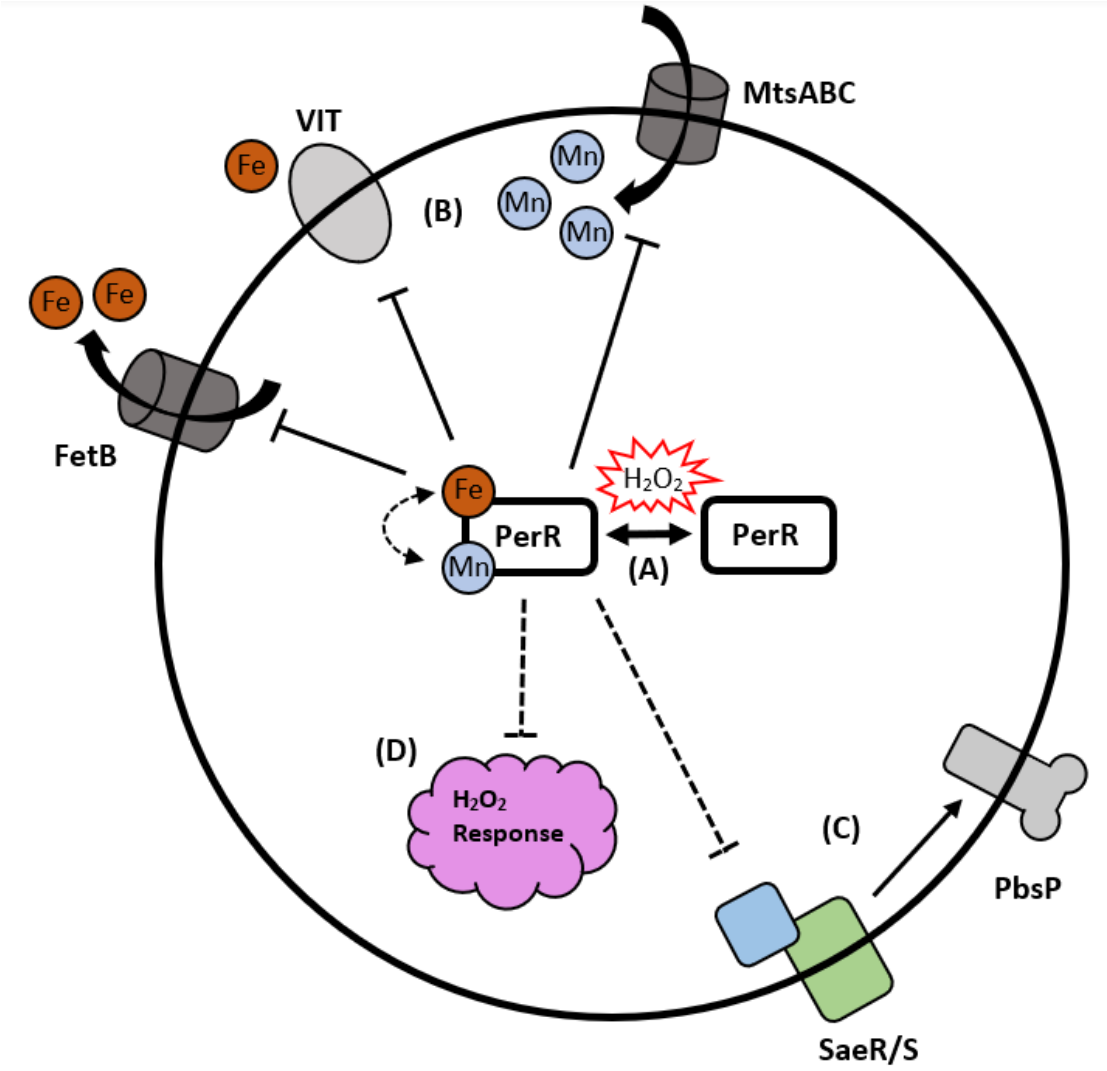

Figure 17: Proposed *perR* regulon in Group B *streptococcus*
(A) PerR protein is bound to either an Fe or Mn metal cofactor when functioning as a repressor binding to DNA and inhibiting transcription. Interaction with H_2O_2 results in change in protein structure and de-repression. (B) H_2O_2 stress results in de-repression of the *MtsABC* Mn transporter, *fetB*, a putative iron exporter, and the uncharacterized *VIT* family iron transporter, resulting in changes to intracellular metal concentrations. (C) *PerR* also negatively regulates the *saeR/S* two component system, although it is unknown if it is direct or indirect regulation. *SaeR/S* in turn positively regulates the membrane associated virulence factor *pbsP*. (D) *PerR* is also responsible for the regulation of systems important for the response of GBS to H_2O_2, though it has not been identified if these systems are driven by DNA repair, H_2O_2 breakdown, or metal homeostasis.

complement, as stability of the plasmid vector in the GBS population in a murine model was unknown. Vaginal colonization conducted with CJB111 WT and Δ*perR* strains in the CD-1 mouse line, mirroring the conditions of the *Krmit* tnseq, did see decreased ability to colonize by the Δ*perR* strain as predicted be underrepresentation of *perR* transposon mutants in the Tnseq experiment following colonization. However, this phenotype was not maintained in the A909 background, or in C57BL/6 mice. One A909 colonization experiment in C57BL/6 N sourced from Inotiv even showed increased colonization by the Δ*perR* strain in uterine tissues, though no difference in bacterial burden in other tissues. However, in a second A909 colonization experiment we used C57BL/6 conducted in C57BL/6 mice sourced from Jackson Laboratory. While this study still produced valuable data, indicating no difference between WT and Δ*perR* strains in vaginal colonization, the slightly different animal line and different source makes a true comparison difficult. It has also been shown that animals from specific laboratories can have their own established microbiomes. Mice have native vaginal microbiomes, and the species present can vary across breeding company and mouse line. It has been observed that CD-1 mice are more often dominated by *Enterobacteriaceae* and *Proteus* species, while C57BL/6 are more commonly associated with colonization by Gram-positive species like *Staphylococcus, Enterococcus,* and *Lactobacillus* (Burcham 2022, Vrbanac 2018). While this line of research will continue to attempt to characterize the reason for the different phenotypes observed, the variability across mouse lines indicates that *perR* is most likely not a primary virulence factor in vaginal colonization and persistence. One possible explanation for the variability seen is that *perR* is an influencing factor in a microbiome dependent manner, impacting vaginal persistence in some microbiome contexts but not others.

Given the relevance of GBS systemic disease in maternal-fetal health and those with comorbidities, we also used a murine model of systemic disease to test the role of *perR* in this host niche. In both A909 and CJB111 backgrounds the Δ*perR* strains showed significant decreases in virulence. This was observed by animal survival, as well as health scores of animals over the course of an experiment and bacterial burden in tissues following animal euthanasia. This is consistent with our hypothesis that *perR* is a regulator of iron homeostasis, as the importance of iron acquisition and balance in disease has been shown in both GBS (Joubert 2017) and related GAS (Song 2018, Macdonald 2023). To try to begin to answer if the virulence defect in the Δ*perR* strains was caused by a reduction in ability to evade or survive the host immune system, a neutrophil depletion model infected with CJB111 was used. While both WT and Δ*perR* strains showed increased virulence in the depletion mice (WT as measured by survival, Δ*perR* mice measured by health score as all Δ*perR* infected mice survived), neutrophil depletion did not restore Δ*perR* virulence closer to WT levels, indicating immune sensitivity to neutrophils is not the source of the Δ*perR* strains decreased virulence in a systemic system. It is also worth noting that while these models are valuable for studying GBS in the context of a mammalian host, it is important to note the limitations of these models. Concerning vaginal colonization especially, differences in murine hormonal regulation, vaginal microbiome and vaginal pH should all be acknowledged (McCracken 2021).

To better understand why a significant decrease in virulence was observed in Δ*perR* strains in a systemic context, but a corresponding decrease in vaginal colonization was not observed, bacteria were grown in blood from healthy donors to test if a *perR* deletion also resulted in decreased survival in this environment. In both backgrounds most bacteria were cleared from blood within 6 hours, and no strain dependent difference was observed between

WT/pABG5, Δ*perR*/pABG5, or Δ*perR*/pABG5:*perR* strains in either background. This difference from results seen in a murine systemic model may be caused by several different factors. First, the immune profile of human and mouse blood is quite different. Human blood is rich in neutrophils, which make up 50-70% of circulating immune cells, while lymphocytes typically make up the minority. However, in mouse blood 75-90% of immune cells are lymphocytes, with neutrophils making up only a small percentage (Mestas 2004). Additionally, blood taken from healthy donors does not accurately represent elderly and immune compromised populations where GBS infection is most likely to occur.

Future Directions

We have demonstrated that *perR* in GBS functions as a regulator that impacts both ROS stress and iron homeostasis. However, the specifics of its metal binding interactions, as well as its direct impact on intracellular metals, are still uncharacterized. We propose using Isothermal Titration Calorimetry (ITC) to more clearly identify the interactions between PerR protein and zinc, manganese and iron ions. Inductively Coupled Plasma Mass Spectrometry (ICP-MS) will also be used to identify the impact of *perR* deletion on intracellular metal contents. Vaginal colonization models will also be repeated in the A909 background to identify if mouse vender differences drove the changes observed in the two A909 WT and Δ*perR* colonization experiments conducted.

While significant work has been conducted in characterizing the regulon of *perR* and identifying its impact on persistence in two specific host niches, the specific mechanisms of decreased virulence in a systemic model remains unknown. Given the role of *perR* as an iron regulator conducting systemic infection models in β-2-microglobulin (β2m) knockout mice, which show increased iron levels, or lactoferrin knockout mice, which lack the iron binding and

sequestration protein lactoferrin, could help elucidate if the virulence decrease of a Δ*perR* strain is caused by the inability to properly regulate iron homeostasis.

Additionally, this work provides several avenues for further study into the metal regulatory systems of GBS. Both *fetB* and *VIT* are putatively involved in iron import or export based on sequence homology, and it could be that these genes, or some other combination of genes within the *perR* regulon are responsible for observed virulence differences. Characterization of genes identified in this study will also further the understanding of the GBS ROS response and its interplay with metal homeostasis. The interesting downregulation of numerous prophage associated genes identified in A909 shown by RNAseq also poses interesting questions regarding the role of these phage elements in GBS to investigate at a later stage.

References

1. Abramson, J., Adler, J., Dunger, J. et al. Accurate structure prediction of biomolecular interactions with AlphaFold 3. Nature 630, 493–500 (2024). https://doi.org/10.1038/s41586-024-07487-w
2. Adrian L. Watson, Jeremy N. Skepper, Eric Jauniaux, Graham J. Burton, Susceptibility of Human Placental Syncytiotrophoblastic Mitochondria to Oxygen-Mediated Damage in Relation to Gestational Age, The Journal of Clinical Endocrinology & Metabolism, Volume 83, Issue 5, 1 May 1998, Pages 1697–1705, https://doi.org/10.1210/jcem.83.5.4830
3. American College of Obstetricians and Gynecologists. (2020). Prevention of group B streptococcal early-onset disease in newborns (ACOG Committee Opinion No. 797). Obstetrics & Gynecology, 135(2), e51–e72. https://doi.org/10.1097/AOG.0000000000003668
4. Armistead B, Oler E, Adams Waldorf K, Rajagopal L. The Double Life of Group B Streptococcus: Asymptomatic Colonizer and Potent Pathogen. J Mol Biol. 2019 Jul 26;431(16):2914-2931. doi: 10.1016/j.jmb.2019.01.035. Epub 2019 Jan 31. PMID: 30711542; PMCID: PMC6646060.
5. Baichoo N, Helmann JD. Recognition of DNA by Fur: a reinterpretation of the Fur box consensus sequence. J Bacteriol. 2002 Nov;184(21):5826-32. doi: 10.1128/JB.184.21.5826-5832.2002. PMID: 12374814; PMCID: PMC135393.
6. Banerjee, A. et al. Bacterial Pili exploit integrin machinery to promote immune activation and efficient blood-brain barrier penetration. Nat. Commun. 2:462 doi: 10.1038/ncomms1474 (2011).

7. Bebien M, Hensler ME, Davanture S, Hsu L-C, Karin M, Park JM, et al. (2012) The Pore-Forming Toxin β hemolysin/cytolysin Triggers p38 MAPK-Dependent IL-10 Production in Macrophages and Inhibits Innate Immunity. PLoS Pathog 8(7): e1002812. https://doi.org/10.1371/journal.ppat.1002812
8. Berardi A, Trevisani V, Di Caprio A, Bua J, China M, Perrone B, Pagano R, Lucaccioni L, Fanaro S, Iughetti L, Lugli L, Creti R. Understanding Factors in Group B Streptococcus Late-Onset Disease. Infect Drug Resist. 2021 Aug 17;14:3207-3218. doi: 10.2147/IDR.S291511. PMID: 34429620; PMCID: PMC8380284.
9. Björklund V, Saxén H, Hertting O, Malchau Carlsen EL, Hoffmann S, Håkansson S, Stefánsson Thors V, Haraldsson Á, Brigtsen AK, Döllner H, Huhtamäki H, Pokka T, Ruuska TS; Nordic Research Network for Paediatric Infectious Diseases Study Group (NORDPID). Early-onset group B streptococcal infections in five Nordic countries with different prevention policies, 1995 to 2019. Euro Surveill. 2024 Jan;29(3):2300193. doi: 10.2807/1560-7917.ES.2024.29.3.2300193. PMID: 38240058; PMCID: PMC10797658.
10. Bray, B.A., Sutcliffe, I.C. & Harrington, D.J. Expression of the MtsA lipoprotein of Streptococcus agalactiae A909 is regulated by manganese and iron. Antonie van Leeuwenhoek 95, 101–109 (2009). https://doi.org/10.1007/s10482-008-9291-6
11. Brenot, A., King, K.Y. and Caparon, M.G. (2005), The PerR regulon in peroxide resistance and virulence of Streptococcus pyogenes. Molecular Microbiology, 55: 221-234. https://doi.org/10.1111/j.1365-2958.2004.04370.x
12. Burcham LR, Akbari MS, Alhajjar N, Keogh RA, Radin JN, Kehl-Fie TE,Belew AT,El-Sayed NM,McIver KS, Doran KS. 2022. Genomic Analyses Identify Manganese

Homeostasis as a Driver of Group B Streptococcal Vaginal Colonization. mBio 13:e00985-22. https://doi.org/10.1128/mbio.00985-22

13. Burcham LR, Bath JR, Werlang CA, Lyon LM, Liu N, Evans C, Ribbeck K, Doran KS. Role of MUC5B during Group B Streptococcal Vaginal Colonization. mBio. 2022 Apr 26;13(2):e0003922. doi: 10.1128/mbio.00039-22. Epub 2022 Mar 24. PMID: 35323039; PMCID: PMC9040740.
14. Burcham LR,Burcham ZM,Akbari MS, Metcalf JL, Doran KS. 2022. Interrelated Effects of Zinc Deficiency and the Microbiome on Group B Streptococcal Vaginal Colonization. mSphere 7:e00264-22. https://doi.org/10.1128/msphere.00264-22
15. Buscetta M, Firon A, Pietrocola G, et al. 2016; PbsP, a cell wall-anchored protein that binds plasminogen to promote hematogenous dissemination of group B Streptococcus. Molecular Microbiology, 101(1), 27–41. https://doi.org/10.1111/mmi.13357
16. Cape, Alison MD; Tuomala, Ruth E. MD; Taylor, Chirisse MPH; Puopolo, Karen M. MD, PhD. Peripartum Bacteremia in the Era of Group B Streptococcus Prophylaxis. Obstetrics & Gynecology 121(4):p 812-818, April 2013. | DOI: 10.1097/AOG.0b013e3182888032
17. Carlin, A. F., Uchiyama, S., Chang, Y. C., Lewis, A. L., Nizet, V., & Varki, A. (2009). Molecular mimicry of host sialylated glycans allows a bacterial pathogen to engage neutrophil Siglec-9 and dampen the innate immune response. Blood, 113(14), 3333-3336
18. Cassidy-Bushrow AE, Sitarik A, Levin AM, Lynch SV, Havstad S, Ownby DR, Johnson CC, Wegienka G. Maternal group B Streptococcus and the infant gut microbiota. J Dev Orig Health Dis. 2016 Feb;7(1):45-53. doi: 10.1017/S2040174415001361. Epub 2015 Aug 12. PMID: 26264560; PMCID: PMC4847528.

19. Chaguza C, Jamrozy D, Bijlsma MW, Kuijpers TW, van de Beek D, van der Ende A, Bentley SD. Population genomics of Group B Streptococcus reveals the genetics of neonatal disease onset and meningeal invasion. Nat Commun. 2022 Jul 21;13(1):4215. doi: 10.1038/s41467-022-31858-4. PMID: 35864107; PMCID: PMC9304382.
20. Chang Y-C, Olson J, Beasley FC, Tung C, Zhang J, Crocker PR, et al. (2014) Group B Streptococcus Engages an Inhibitory Siglec through Sialic Acid Mimicry to Blunt Innate Immune and Inflammatory Responses In Vivo. PLoS Pathog 10(1): e1003846. https://doi.org/10.1371/journal.ppat.1003846
21. Chen Z, Zhang Z, Zhang H, Xie B. Analysis of the Oxidative Stress Status in Nonspecific Vaginitis and Its Role in Vaginal Epithelial Cells Apoptosis. Biomed Res Int. 2015;2015:795656. doi: 10.1155/2015/795656. Epub 2015 Oct 19. PMID: 26558281; PMCID: PMC4628999
22. Chen Z, Zhang Z, Zhang H, Xie B. Analysis of the Oxidative Stress Status in Nonspecific Vaginitis and Its Role in Vaginal Epithelial Cells Apoptosis. Biomed Res Int. 2015;2015:795656. doi: 10.1155/2015/795656. Epub 2015 Oct 19. PMID: 26558281; PMCID: PMC4628999.
23. Cherpes TL, Hillier SL, Meyn LA, Busch JL, Krohn MA. A delicate balance: risk factors for acquisition of bacterial vaginosis include sexual activity, absence of hydrogen peroxide-producing lactobacilli, black race, and positive herpes simplex virus type 2 serology. Sex Transm Dis. 2008 Jan;35(1):78-83. doi: 10.1097/OLQ.0b013e318156a5d0. PMID: 17989585.
24. Cieslewicz MJ, Chaffin D, Glusman G, Kasper D, Madan A, Rodrigues S, Fahey J, Wessels MR, Rubens CE. Structural and genetic diversity of group B streptococcus capsular

polysaccharides. Infect Immun. 2005 May;73(5):3096-103. doi: 10.1128/IAI.73.5.3096-3103.2005. PMID: 15845517; PMCID: PMC1087335.

25. Cook LCC, Hu H, Maienschein-Cline M, Federle MJ. 2018. A Vaginal Tract Signal Detected by the Group B Streptococcus SaeRS System Elicits Transcriptomic Changes and Enhances Murine Colonization. Infect Immun 86:10.1128/iai.00762-17. https://doi.org/10.1128/iai.00762-17
26. Coppolino F, De Gaetano GV, Claverie C, Sismeiro O, Varet H, Legendre R, Pellegrini A, Berbiglia A, Tavella L, Lentini G, Famà A, Barbieri G, Pietrocola G, Teti G, Firon A, Beninati C. The SaeRS two-component system regulates virulence gene expression in group B *Streptococcus* during invasive infection. mBio. 2024 Sep 11;15(9):e0197524. doi: 10.1128/mbio.01975-24. Epub 2024 Aug 19. PMID: 39158291; PMCID: PMC11389388.
27. da Conceição Mendonça J, Lumsdaine S, Burcham LR. 2025. Comparison of lateral tail vein and retro-orbital venous sinus as routes of inoculation to study Group B streptococcal systemic infection. Microbiol Spectr 13:e02104-24. https://doi.org/10.1128/spectrum.02104-24
28. De Gaetano, G. V., Pietrocola, G., Romeo, L., Galbo, R., Lentini, G., Giardina, M., Biondo, C., Midiri, A., Mancuso, G., Venza, M., Venza, I., Firon, A., Trieu-Cuot, P., Teti, G., Speziale, P., & Beninati, C. (2018). The Streptococcus agalactiae cell wall-anchored protein PbsP mediates adhesion to and invasion of epithelial cells by exploiting the host vitronectin/αv integrin axis. Molecular Microbiology, 110(1), 82-94
29. Doran, K. S., Liu, G. Y., & Nizet, V. (2003). Group B streptococcal β-hemolysin/cytolysin activates neutrophil signaling pathways in brain endothelium and contributes to development of meningitis. Journal of Clinical Investigation, 112(5), 736-744

30. Elizabeth A. Veal, Paraskevi Kritsiligkou. How are hydrogen peroxide messages relayed to affect cell signalling?,Current Opinion in Chemical Biology,Volume 81,2024,102496, ISSN 1367-5931, https://doi.org/10.1016/j.cbpa.2024.102496.
31. Faralla C, Metruccio MMDe Chiara M, Mu R, Patras KA, Muzzi A, Grandi G, Margarit I, Doran KS, Janulczyk R. 2014. Analysis of Two-Component Systems in Group B Streptococcus Shows That RgfAC and the Novel FspSR Modulate Virulence and Bacterial Fitness. mBio 5:10.1128/mbio.00870-14. https://doi.org/10.1128/mbio.00870-14
32. Fernandez A, Lechardeur D, Derré-Bobillot A, Couvé E, Gaudu P, Gruss A (2010) Two Coregulated Efflux Transporters Modulate Intracellular Heme and Protoporphyrin IX Availability in Streptococcus agalactiae. PLoS Pathog 6(4): e1000860. https://doi.org/10.1371/journal.ppat.1000860
33. Fiorella Bianchi-Jassir, Proma Paul, Ka-Ning To, Clara Carreras-Abad, Anna C. Seale, Elita Jauneikaite, Shabir A. Madhi, Neal J. Russell, Jenny Hall, Lola Madrid, Quique Bassat, Gaurav Kwatra, Kirsty Le Doare, Joy E. Lawn, "Systematic review of Group B Streptococcal capsular types, sequence types and surface proteins as potential vaccine candidates," Vaccine, Volume 38, Issue 43, 2020, Pages 6682-6694, ISSN 0264-410X, https://doi.org/10.1016/j.vaccine.2020.08.052.
34. Fuangthong M, Herbig AF, Bsat N, Helmann JD 2002. Regulation of the Bacillus subtilis fur and perR Genes by PerR: Not All Members of the PerR Regulon Are Peroxide Inducible. J Bacteriol 184:. https://doi.org/10.1128/jb.184.12.3276-3286.2002
35. Ge, R., Sun, X. & He, Q. Iron acquisition by Streptococcus species: An updated review. Front. Biol. China 4, 392–401 (2009). https://doi.org/10.1007/s11515-009-0035-4

36. Giedroc DP. Hydrogen peroxide sensing in Bacillus subtilis: it is all about the (metallo)regulator. Mol Microbiol. 2009 Jul;73(1):1-4. doi: 10.1111/j.1365-2958.2009.06752.x. Epub 2009 Jun 8. PMID: 19508286; PMCID: PMC2765198.

37. Goh KGK, Desai D, Thapa R, Prince D, Acharya D, Sullivan MJ, Ulett GC. An opportunistic pathogen under stress: how Group B Streptococcus responds to cytotoxic reactive species and conditions of metal ion imbalance to survive. FEMS Microbiol Rev. 2024 May 8;48(3):fuae009. doi: 10.1093/femsre/fuae009. PMID: 38678005; PMCID: PMC11098048.

38. Granok AB Parsonage D, Ross RP, Caparon MG 2000. The RofA Binding Site in Streptococcus pyogenes Is Utilized in Multiple Transcriptional Pathways. J Bacteriol 182:. https://doi.org/10.1128/jb.182.6.1529-1540.2000

39. Grifantini R, Toukoki C, Colaprico A, Gryllos I. Peroxide stimulon and role of PerR in group A Streptococcus. J Bacteriol. 2011 Dec;193(23):6539-51. doi: 10.1128/JB.05924-11. Epub 2011 Sep 23. PMID: 21949080; PMCID: PMC3232902.

40. Helmann JDWu MFW, Gaballa A, Kobel PAMorshedi MM, Fawcett P, Paddon C 2003. The Global Transcriptional Response of Bacillus subtilis to Peroxide Stress Is Coordinated by Three Transcription Factors. J Bacteriol 185:. https://doi.org/10.1128/jb.185.1.243-253.2003

41. Herbig, A. F., & Helmann, J. D. (2002). Roles of metal ions and hydrogen peroxide in modulating the interaction of the Bacillus subtilis PerR peroxide regulon repressor with operator DNA. Molecular Microbiology, 41(4), 849-859

42. Jackson L.W, Schisterman E.F, Dey-Rao R, Browne R, Armstrong D, Oxidative stress and endometriosis, Human Reproduction, Volume 20, Issue 7, 1 July 2005, Pages 2014–2020, https://doi.org/10.1093/humrep/dei001

43. Jackson L.W, Schisterman E.F, Dey-Rao R, Browne R, Armstrong D, Oxidative stress and endometriosis, Human Reproduction, Volume 20, Issue 7, 1 July 2005, Pages 2014–2020, https://doi.org/10.1093/humrep/dei001

44. Ji CJ, Kim JH, Won YB, Lee YE, Choi TW, Ju SY, Youn H, Helmann JD, Lee JW. Staphylococcus aureus PerR Is a Hypersensitive Hydrogen Peroxide Sensor using Iron-mediated Histidine Oxidation. J Biol Chem. 2015 Aug 14;290(33):20374-86. doi: 10.1074/jbc.M115.664961. Epub 2015 Jul 1. PMID: 26134568; PMCID: PMC4536443.

45. Jiang S, Ishmael N, Hotopp JD, Puliti M, Tissi L, Kumar N, Cieslewicz MJTettelin H, Wessels MR 2008. Variation in the Group B Streptococcus CsrRS Regulon and Effects on Pathogenicity. J Bacteriol 190:. https://doi.org/10.1128/jb.01677-07

46. Jiang SPark SEYadav PPaoletti LC, Wessels MR 2012. Regulation and Function of Pilus Island 1 in Group B Streptococcus. J Bacteriol 194:. https://doi.org/10.1128/jb.00202-12

47. Joubert, L. et al. Visualization of the role of host heme on the virulence of the heme auxotroph Streptococcus agalactiae. Sci. Rep. 7, 40435; doi: 10.1038/srep40435 (2017).

48. K A Patras, B Rösler, M L Thoman, K S Doran, Characterization of host immunity during persistent vaginal colonization by Group B Streptococcus, Mucosal Immunology, Volume 8, Issue 6, 2015, Pages 1339-1348, ISSN 1933-0219, https://doi.org/10.1038/mi.2015.23. (https://www.sciencedirect.com/science/article/pii/S193302192201011X)

49. Kapatai G, Patel D, Efstratiou A, Chalker VJ. Comparison of molecular serotyping approaches of Streptococcus agalactiae from genomic sequences. BMC Genomics. 2017 Jun 1;18(1):429. doi: 10.1186/s12864-017-3820-5. PMID: 28571573; PMCID: PMC5455115.

50. Kathryn A Patras, Jaclyn Derieux, Mahmoud M Al-Bassam, Nichole Adiletta, Alison Vrbanac, John D Lapek, Karsten Zengler, David J Gonzalez, Victor Nizet, Group

B *Streptococcus* Biofilm Regulatory Protein A Contributes to Bacterial Physiology and Innate Immune Resistance, *The Journal of Infectious Diseases,* Volume 218, Issue 10, 15 November 2018, Pages 1641–1652, https://doi.org/10.1093/infdis/jiy341

51. King KY, Horenstein JA, Caparon MG. 2000. Aerotolerance and Peroxide Resistance in Peroxidase and PerR Mutants of Streptococcus pyogenes. J Bacteriol 182:. https://doi.org/10.1128/jb.182.19.5290-5299.2000
52. Korir ML, Flaherty RA, Rogers LM, Gaddy JA, Aronoff DM, Manning SD. Investigation of the Role That NADH Peroxidase Plays in Oxidative Stress Survival in Group B Streptococcus. Front Microbiol. 2018 Nov 20;9:2786. doi: 10.3389/fmicb.2018.02786. PMID: 30515142; PMCID: PMC6255910.
53. Lawn, J. E., Bianchi-Jassir, F., Russell, N. J., Seale, A. C., Baker, C. J., Bartlett, L., Cutland, C., Gravett, M. G., Heath, P. T., Ip, M., Madhi, S. A., Rubens, C. E., Saha, S. K., Schrag, S. J., Stoll, B. J., Vekemans, J., & Sobanjo-Ter Meulen, A. (2022). Group B streptococcus infection during pregnancy and infancy: estimates of regional and global burden. The Lancet Global Health, 10(6), e807–e819. https://doi.org/10.1016/S2214-109X(22)00093-6
54. Lechardeur, D., Fernandez, A., Robert, B., Gaudu, P., Trieu-Cuot, P., Lamberet, G., & Gruss, A. (2010). The 2-Cys peroxiredoxin alkyl hydroperoxide reductase C binds heme and participates in its intracellular availability in Streptococcus agalactiae. Journal of Biological Chemistry, 285(21), 16032-16041.
55. Lee, JW., Helmann, J.D. Functional specialization within the Fur family of metalloregulators. Biometals 20, 485–499 (2007). https://doi.org/10.1007/s10534-006-9070-7

56. Lentini, G., Midiri, A., Firon, A. et al. The plasminogen binding protein PbsP is required for brain invasion by hypervirulent CC17 Group B streptococci. Sci Rep 8, 14322 (2018). https://doi.org/10.1038/s41598-018-32774-8

57. Li H, Zhou X, Huang Y, Liao B, Cheng L and Ren B (2021) Reactive Oxygen Species in Pathogen Clearance: The Killing Mechanisms, the Adaption Response, and the Side Effects. Front. Microbiol. 11:622534. doi: 10.3389/fmicb.2020.622534

58. Li S, Liang Q, Qing W, Fang Z, Yuan C, Pan S, Xie H, Li X, Chen M, He Y, Zhou H, Wang Q. Maternal group B Streptococcus decreases infant length and alters the early-life microbiome: a prospective cohort study. Ann Med. 2025 Dec;57(1):2442070. doi: 10.1080/07853890.2024.2442070. Epub 2024 Dec 18. PMID: 39693119; PMCID: PMC11656753.

59. Liu Y and Ai H (2024) Current research update on group B streptococcal infection related to obstetrics and gynecology. *Front. Pharmacol.* 15:1395673. doi: 10.3389/fphar.2024.1395673

60. Liu, G. Y., Doran, K. S., & Lawrence, T. (2004). Sword and shield: Linked group B streptococcal β-hemolysin/cytolysin and carotenoid pigment function to subvert host phagocyte defense. *Proceedings of the National Academy of Sciences*, 101(40), 14491–14496. https://doi.org/10.1073/pnas.0406143101

61. Lu, J., Wang, Z., Cao, J. et al. A novel and compact review on the role of oxidative stress in female reproduction. Reprod Biol Endocrinol 16, 80 (2018). https://doi.org/10.1186/s12958-018-0391-5

62. Makthal N, Rastegari S, Sanson M, Ma Z, Olsen RJ, Helmann JD, Musser JM, Kumaraswami M. Crystal structure of peroxide stress regulator from Streptococcus pyogenes provides functional insights into the mechanism of oxidative stress sensing. J Biol Chem.

2013 Jun 21;288(25):18311-24. doi: 10.1074/jbc.M113.456590. Epub 2013 May 3. PMID: 23645680; PMCID: PMC3689973.

63. Margarit I. et al. Preventing Bacterial Infections with Pilus-Based Vaccines: the Group B Streptococcus Paradigm, The Journal of Infectious Diseases, Volume 199, Issue 1, 1 January 2009, Pages 108–115, https://doi.org/10.1086/595564

64. Martínez, L.E.; Gómez, G.; Ramírez, N.; Franco, B.; Robleto, E.A.; Pedraza-Reyes, M. 8-OxoG-Dependent Regulation of Global Protein Responses Leads to Mutagenesis and Stress Survival in Bacillus subtilis. Antioxidants 2024, 13, 332. https://doi.org/10.3390/antiox13030332

65. McCracken JM, Calderon GA, Robinson AJ, Sullivan CN, Cosgriff-Hernandez E, Hakim JCE. Animal Models and Alternatives in Vaginal Research: a Comparative Review. Reprod Sci. 2021 Jun;28(6):1759-1773. doi: 10.1007/s43032-021-00529-y. Epub 2021 Apr 6. PMID: 33825165; PMCID: PMC8204935.

66. McLaughlin JM, Peyrani P, Furmanek S, Khan FL, Quinn A, Jodar L, Ramirez J, Swerdlow DL. Burden of Adults Hospitalized With Group B Streptococcal Infection. J Infect Dis. 2021 Oct 13;224(7):1170-1178. doi: 10.1093/infdis/jiaa110. PMID: 32188975; PMCID: PMC8561246.

67. Megli, C. J., Carlin, S. M., Giacobe, E. J., & Hillebrand, E. M. (2025). Virulence and pathogenicity of group B Streptococcus: Virulence factors and their roles in perinatal infection. Virulence, 16(1), 2451173.

68. Mestas, J., Huges, C.C.W. (2004). Of Mice and Not Men: Differences between Mouse and Human Immunology. J Immunol 1 March 2004; 172 (5): 2731–2738. https://doi.org/10.4049/jimmunol.172.5.2731

69. Morgan JA, Zafar N, Cooper DB. Group B Streptococcus and Pregnancy. [Updated 2024 Aug 11]. In: StatPearls [Internet]. Treasure Island (FL): StatPearls Publishing; 2025 Jan-. Available from: https://www.ncbi.nlm.nih.gov/books/NBK482443/

70. Nai-Yu Wang, Kathryn A. Patras, Ho Seong Seo, Courtney K. Cavaco, Berenice Rösler, Melody N. Neely, Paul M. Sullam, Kelly S. Doran, Group B Streptococcal Serine-Rich Repeat Proteins Promote Interaction With Fibrinogen and Vaginal Colonization, *The Journal of Infectious Diseases*, Volume 210, Issue 6, 15 September 2014, Pages 982–991, https://doi.org/10.1093/infdis/jiu151

71. Nathan C, Cunningham-Bussel A. Beyond oxidative stress: an immunologist's guide to reactive oxygen species. Nat Rev Immunol. 2013 May;13(5):349-61. doi: 10.1038/nri3423. PMID: 23618831; PMCID: PMC4250048.

72. Nicolaou SA, Fast AG, Nakamaru-Ogiso E, Papoutsakis ET. Overexpression of fetA (ybbL) and fetB (ybbM), Encoding an Iron Exporter, Enhances Resistance to Oxidative Stress in Escherichia coli. Appl Environ Microbiol. 2013 Dec;79(23):7210-9. doi: 10.1128/AEM.02322-13. Epub 2013 Sep 13. PMID: 24038693; PMCID: PMC3837747.

73. O'Hanlon DE, Moench TR, Cone RA (2013) Vaginal pH and Microbicidal Lactic Acid When Lactobacilli Dominate the Microbiota. PLoS ONE 8(11): e80074. https://doi.org/10.1371/journal.pone.0080074

74. O'Hanlon, D.E., Lanier, B.R., Moench, T.R. et al. Cervicovaginal fluid and semen block the microbicidal activity of hydrogen peroxide produced by vaginal lactobacilli. BMC Infect Dis 10, 120 (2010). https://doi.org/10.1186/1471-2334-10-120

75. Palacio J R , Iborra A, Ulcova-Gallova Z, Badia R , Martínez P, The presence of antibodies to oxidative modified proteins in serum from polycystic ovary syndrome patients, Clinical

and Experimental Immunology, Volume 144, Issue 2, May 2006, Pages 217–222, https://doi.org/10.1111/j.1365-2249.2006.03061.x

76. Palacio J R, Iborra A, Ulcova-Gallova Z, Badia R, Martínez P, The presence of antibodies to oxidative modified proteins in serum from polycystic ovary syndrome patients, Clinical and Experimental Immunology, Volume 144, Issue 2, May 2006, Pages 217–222, https://doi.org/10.1111/j.1365-2249.2006.03061.x
77. Palyada, K., Sun, YQ., Flint, A. *et al.* Characterization of the oxidative stress stimulon and PerR regulon of *Campylobacter jejuni*. *BMC Genomics* **10**, 481 (2009). https://doi.org/10.1186/1471-2164-10-481
78. Patras KA, Doran KS. A Murine Model of Group B Streptococcus Vaginal Colonization. J Vis Exp. 2016 Nov 16;(117):54708. doi: 10.3791/54708. PMID: 27911391; PMCID: PMC5226234.
79. Peng W,Yang X,Wang N,Gao T, Liu Z, Liu W, Zhou D, Yang K, Guo R, Liang W, Chen H,Tian Y, Yuan F, Bei W,, 2022. PerR-Regulated Manganese Import Contributes to Oxidative Stress Defense in Streptococcus suis. Appl Environ Microbiol 88:e00086-22. https://doi.org/10.1128/aem.00086-22
80. R. Macdonald,B.J. Mahoney,J. Soule,A.K. Goring,J. Ford,J.A. Loo,D. Cascio,& R.T. Clubb, The Shr receptor from Streptococcus pyogenes uses a cap and release mechanism to acquire heme–iron from human hemoglobin, Proc. Natl. Acad. Sci. U.S.A. 120 (5) e2211939120, https://doi.org/10.1073/pnas.2211939120 (2023).
81. Raabe VN.Shane AL. 2019. Group B *Streptococcus* (*Streptococcus agalactiae*). Microbiol Spectr 7:10.1128/microbiolspec.gpp3-0007-2018.https://doi.org/10.1128/microbiolspec.gpp3-0007-2018

82. Randis, T. M., Gelber, S. E., Hooven, T. A., Abellar, R. G., Akabas, L. H., Lewis, E. L., ... & Ratner, A. J. (2014). Group B Streptococcus β-hemolysin/Cytolysin breaches maternal-fetal barriers to cause preterm birth and intrauterine fetal demise in vivo. Journal of Infectious Diseases, 210(2), 265–273. https://doi.org/10.1093/infdis/jiu067

83. Ricci SJanulczyk R, Björck L. 2002. The Regulator PerR Is Involved in Oxidative Stress Response and Iron Homeostasis and Is Necessary for Full Virulence of Streptococcus pyogenes. Infect Immun 70:. https://doi.org/10.1128/iai.70.9.4968-4976.2002

84. Ricci SJanulczyk R, Björck L. 2002. The Regulator PerR Is Involved in Oxidative Stress Response and Iron Homeostasis and Is Necessary for Full Virulence of Streptococcus pyogenes. Infect Immun 70:. https://doi.org/10.1128/iai.70.9.4968-4976.2002

85. Romeo, A. M., Christen, L., Niles, E. G., & Kosman, D. J. (2001). Intracellular chelation of iron by bipyridyl inhibits DNA virus replication: ribonucleotide reductase maturation as a probe of intracellular iron pools. Journal of Biological Chemistry, 276(26), 24301–24308. https://doi.org/10.1074/jbc.M010345200

86. Rosa-Fraile M, Dramsi S, Spellerberg B. Group B streptococcal haemolysin and pigment, a tale of twins. FEMS Microbiol Rev. 2014 Sep;38(5):932-46. doi: 10.1111/1574-6976.12071. Epub 2014 Apr 4. PMID: 24617549; PMCID: PMC4315905.

87. Russell NJ, Seale AC, O'Driscoll M, O'Sullivan C, Bianchi-Jassir F, Gonzalez-Guarin J, Lawn JE, Baker CJ, Bartlett L, Cutland C, Gravett MG, Heath PT, Le Doare K, Madhi SA, Rubens CE, Schrag S, Sobanjo-Ter Meulen A, Vekemans J, Saha SK, Ip M; GBS Maternal Colonization Investigator Group. Maternal Colonization With Group B Streptococcus and Serotype Distribution Worldwide: Systematic Review and Meta-analyses. Clin Infect Dis.

2017 Nov 6;65(suppl_2):S100-S111. doi: 10.1093/cid/cix658. PMID: 29117327; PMCID: PMC5848259.

88. Sachdeva S, Rosett HA, Krischak MK, Weaver KE, Heine RP, Denoble AE, Dotters-Katz SK. Urinary Tract Infection and Progression to Pyelonephritis: Group B Streptococcus versus E. coli. AJP Rep. 2024 Feb 18;14(1):e80-e84. doi: 10.1055/s-0044-1779031. PMID: 38370326; PMCID: PMC10874690.
89. Seixas, A. F., Silva, A. F. Q., Sousa, J. P., Arraiano, C. M., & Andrade, J. M. (2025). The RNA chaperone Hfq is a novel regulator of catalase expression and hydrogen peroxide-induced oxidative stress response in Listeria monocytogenes EGD-e. Molecular Microbiology, 121(6), 1405-1423. https://doi.org/10.1111/mmi.15236
90. Sen A and Imlay JA (2021) How Microbes Defend Themselves From Incoming Hydrogen Peroxide. Front. Immunol. 12:667343. doi: 10.3389/fimmu.2021.667343
91. Sevilla E, Bes MT, Peleato ML, Fillat MF. *Fur-like proteins: Beyond the ferric uptake regulator (Fur) paralog*. Archives of Biochemistry and Biophysics, 701, 108770. https://doi.org/10.1016/j.abb.2021.108770
92. Shabayek, S., Bauer, R., Mauerer, S., Mizaikoff, B. and Spellerberg, B. (2016), A streptococcal NRAMP homologue is crucial for the survival of Streptococcus agalactiae under low pH conditions. Molecular Microbiology, 100: 589-606. https://doi.org/10.1111/mmi.13335
93. Skoff, T. H., Farley, M. M., Petit, S., Craig, A. S., Schaffner, W., Gershman, K., Harrison, L. H., Lynfield, R., Mohle-Boetani, J., Zansky, S., Albanese, B. A., Stefonek, K., Zell, E. R., Jackson, D., Thompson, T., & Schrag, S. J. (2009). Increasing burden of invasive group B

streptococcal disease in nonpregnant adults, 1990-2007. Clinical Infectious Diseases, 49(1), 85-92. https://doi.org/10.1086/599369

94. Song Y, Zhang X, Cai M, Lv C, Zhao Y, Wei D, Zhu H. The Heme Transporter HtsABC of Group A Streptococcus Contributes to Virulence and Innate Immune Evasion in Murine Skin Infections. Front Microbiol. 2018 May 25;9:1105. doi: 10.3389/fmicb.2018.01105. PMID: 29887858; PMCID: PMC5981463.
95. Spencer BL, Deng L, Patras KA, Burcham ZM, Sanches GF, Nagao PE, et al. Cas9 Contributes to Group B Streptococcal Colonization and Disease. Front Microbiol. 2019;10:1930. Epub 2019/09/10. pmid:31497003; PubMed Central PMCID: PMC6712506.
96. Strus, M., Brzychczy-Włoch, M., Gosiewski, T., Kochan, P. and Heczko, P.B. (2006), The in vitro effect of hydrogen peroxide on vaginal microbial communities. FEMS Immunology & Medical Microbiology, 48: 56-63. https://doi.org/10.1111/j.1574-695X.2006.00120.x
97. Sun, X., Ge, R., Chiu, J. F., Sun, H., & He, Q. Y. (2008). Lipoprotein MtsA of MtsABC in Streptococcus pyogenes primarily binds ferrous ion with bicarbonate as a synergistic anion. FEBS Letters, 582(10), 1351-1354
98. Thomas LS, Cook LC. A Novel Conserved Protein in Streptococcus agalactiae, BvaP, Is Important for Vaginal Colonization and Biofilm Formation. mSphere. 2022 Dec 21;7(6):e0042122. doi: 10.1128/msphere.00421-22. Epub 2022 Oct 11. PMID: 36218343; PMCID: PMC9769775.
99. Traoré, D., Ghazouani, A., Jacquamet, L. et al. Structural and functional characterization of 2-oxo-histidine in oxidized PerR protein. Nat Chem Biol 5, 53–59 (2009). https://doi.org/10.1038/nchembio.133

100. Troxell B and Hassan HM (2013) Transcriptional regulation by Ferric Uptake Regulator (Fur) in pathogenic bacteria. Front. Cell. Infect. Microbiol. 3:59. doi: 10.3389/fcimb.2013.00059

101. Ullah I and Lang M (2023) Key players in the regulation of iron homeostasis at the host-pathogen interface. Front. Immunol. 14:1279826. doi: 10.3389/fimmu.2023.1279826

102. Vallor AC, Antonio MA, Hawes SE, Hillier SL. Factors associated with acquisition of, or persistent colonization by, vaginal lactobacilli: role of hydrogen peroxide production. J Infect Dis. 2001 Dec 1;184(11):1431-6. doi: 10.1086/324445. Epub 2001 Oct 30. PMID: 11709785., https://doi.org/10.1086/324445

103. Vrbanac, A., Riestra, A.M., Coady, A. et al. The murine vaginal microbiota and its perturbation by the human pathogen group B Streptococcus. BMC Microbiol 18, 197 (2018). https://doi.org/10.1186/s12866-018-1341-2

104. Waterhouse AM, Procter JB, Martin DMA, Clamp M, Barton GJ (2009) Jalview Version 2 - A multiple sequence alignment editor and analysis workbench. Bioinformatics 25 1189-1191. (doi:10.1093/bioinformatics/btp033)

105. Watson, A. L., Skepper, J. N., Jauniaux, E., & Burton, G. J. (1998). Susceptibility of Human Placental Syncytiotrophoblastic Mitochondria to Oxygen-Mediated Damage in Relation to Gestational Age. The Journal of Clinical Endocrinology & Metabolism, 83(5), 1697-1705.

106. Wilks M, Wiggins R, Whiley A, Hennessy E, Warwick S, Porter H, Corfield A, Millar M. Identification and H(2)O(2) production of vaginal lactobacilli from pregnant women at high risk of preterm birth and relation with outcome. J Clin Microbiol. 2004 Feb;42(2):713-7. doi: 10.1128/JCM.42.2.713-717.2004. PMID: 14766841; PMCID: PMC344438.

107. Yamamoto, Y., Poyart, C., Trieu-Cuot, P., Lamberet, G., Gruss, A., & Gaudu, P. (2005). Respiration metabolism of Group B Streptococcus is activated by environmental haem and quinone and contributes to virulence. Molecular Microbiology, 56(2), 525-534.

108. Yang Y, Luo M, Zhou H, Li C, Luk A, Zhao G, Fung K and Ip M (2019) Role of Two-Component System Response Regulator bceR in the Antimicrobial Resistance, Virulence, Biofilm Formation, and Stress Response of Group B Streptococcus. Front. Microbiol. 10:10. doi: 10.3389/fmicb.2019.00010

Appendix

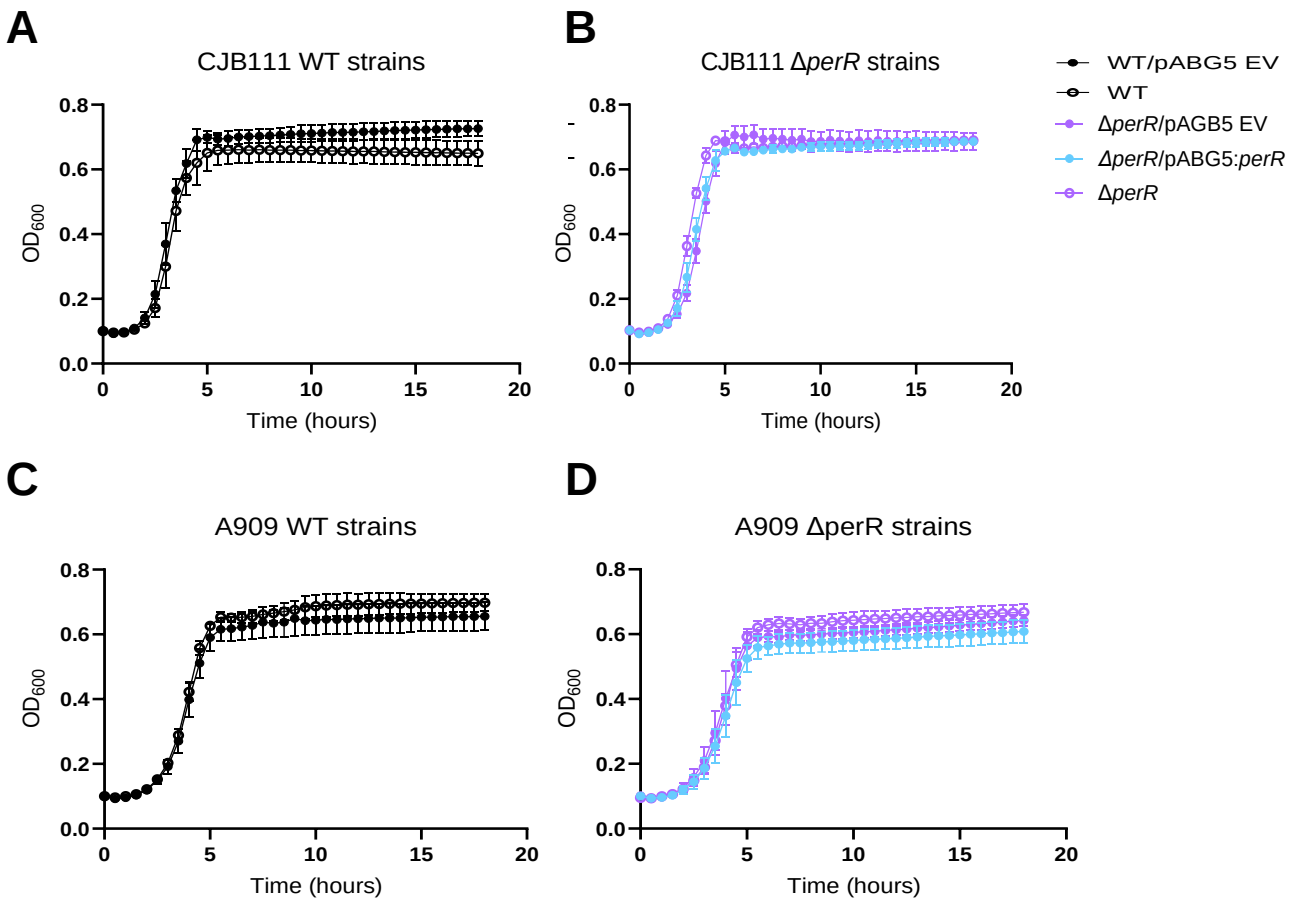

Figure 18: Comparative growth of GBS strains with and without pABG5 plasmid vector CJB111 (A-B) and A909 (C-D) WT and Δ*perR* (red) strain growth in THB compared to growth of the same strains containing either containing a pABG5 empty vector, or pABG5:*perR* expression plasmid (purple). Strains measured on EPOCH2 BioTek plate reader, with timepoints ever 30 minutes.

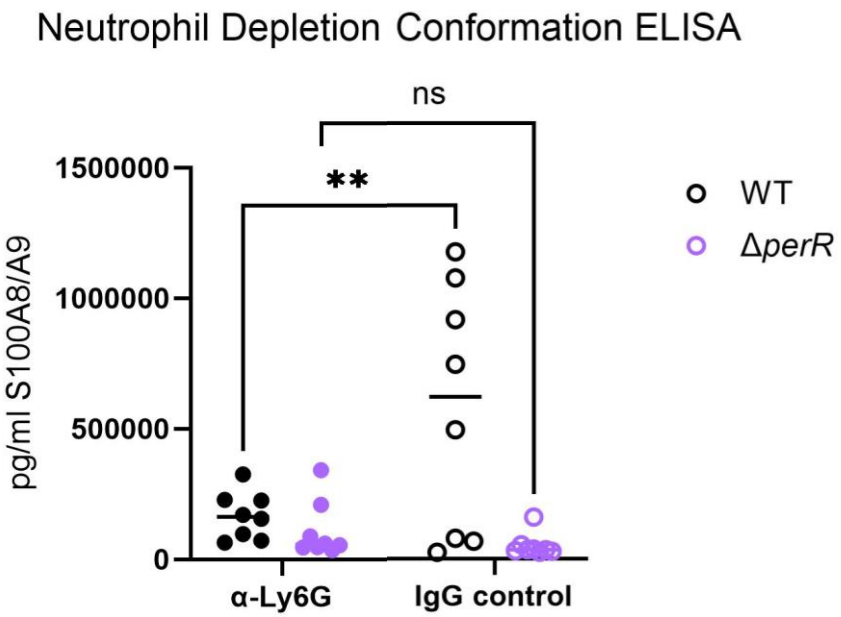

Figure 19: S100A8/A9 ELISA for conformation of mouse neutrophil depletion
S100A8/A9 levels, used as a proxy for neutrophil presence, was measured in mouse brains following neutrophil depletion systemic infection model using R&D Systems™ Mouse S100A8/S100A9 Heterodimer DuoSet ELISA. Data analyzed using two-way ANOVA.

Table 2: Primer List

Primer name	Sequence (5' - 3')	Purpose
LB KanR F	GCCACGTTGTGTCTCAAAATC	Amplification of Kanamycin resistance construct
LB KanR R	CGGTCTGCGTTGTCGG	Amplification of Kanamycin resistance construct
Backbone pHY304 R	TACGAGCCGCGGTGGAGCTCC	Amplification of pHY304 plasmid
Backbone pHY304 F	TGGAAGGAATTCGATATCAAGCTTATCG-ATACC	Amplification of pHY304 plasmid
Up PerR F	GGAGCTCCACCGCGGCTCGTAAACTAGC-GAAGCAATATTG	Amplification of *perR* upstream region
Up PerR R	ATTTTGAGACACAACGTGGCCATAGGAC-TCCTTTCCAGCAC	Amplification of *perR* upstream region
Down PerR F	CTTCCCGACAACGCAGACCGTGAAACGT-AATTGTTCAATCTTTTTTTGTTTCTAG	Amplification of *perR* downstream region
Down PerR R	CTTGATATCGAATTCCTTCCATATCAGTT-GTAATGTGAGG	Amplification of *perR* downstream region
GBS perR F	ACAGTCATTCACATGGTCATAGA	RT-qPCR amplification
GBS *perR* R	GGCAATGTTTAGGTGCTGATG	RT-qPCR amplification
GBS mtsA F	CCAGATGTATGCTGATGGAACT	RT-qPCR amplification
GBS mtsA R	GGTTAGCGATGGAGTTGATGT	RT-qPCR amplification
GBS fetB F	AGCTATTGGGTCAGGGACTA	RT-qPCR amplification

Table 2: Continued

GBS *fetB* R	AACCGCTTGGATAGGTGAAG	RT-qPCR amplification
GBS *VIT* F	CGAGTGCAACTCATAACCTTTG	RT-qPCR amplification
GBS *VIT R*	CAACTGCTGCTTGTTCAGTATC	RT-qPCR amplification
GBS *saeR* F	ACGTTATCTAGAGCAAGCAGGA	RT-qPCR amplification
GBS *saeR* R	AAAGGTTGGTTGGGTTCTCG	RT-qPCR amplification

Primer sequences used for GBS cloning as well as primers used for RT-qPCR targeting *perR, fetB, saeR, VIT,* and *mtsA* expression in GBS. Both forward and reverse primers shown.

Table 3: Predicted PerR Regulated Genes

Gene name/Locus tag	Putative function	*Per*-Box binding site
ID870_02140	class I SAM-dependent methyltransferase	TTTTAATTATTTTAA
ID870_09265	threonine synthase	TTTTAGTTATTGTAA
ID870_08045	TetR/AcrR family transcriptional regulator	TTTTAATTATTTTAA
rimP	ribosome maturation factor RimP	TTATAGTCATTATAA
fetB	ABC transporter ATP-binding protein	TTATAATGATTATAA
queA	tRNA preQ1(34) S-adenosylmethionine ribosyltransferase-isomerase QueA	TTATAATCATTCTAA TTGTAATCATTCTAA
VIT	VIT1/CCC1 transporter family protein	TTATAATCATTCTAA
ID870_04330	ABC transporter permease	TTATAATGATTTTAA
ID870_03055	DUF1836 domain-containing protein	TTTTATTCATTTTAA
mtsA	metal ABC transporter substrate-binding protein	TTATATTAATTTTAA
recA	recombinase RecA	TTCTACTAATTATAA

Table 3: Continued

ID870_10015	type II toxin-antitoxin system RelB/DinJ family antitoxin	TTTTAGTTATTATAA

Genes identified using the consensus *per*-box TTNTANTNATTNTAA in GBS, along with predicted function and *per*-box sequence. Locas tag ID specific to CJB111 (NZ_CP063198) strain.

Vita

Stephen Lumsdaine attended Pellissippi State Community College from August 2016 to 2018 and graduated with an Associates of Science. He then attended the University of Tennessee Knoxville from August 2018 through May 2020 and graduated with a Bachelor of Science degree in biological sciences with a concentration in microbiology, and a minor in philosophy. During his time at UTK, he worked in a research lab studying the mechanisms of *Candida albicans* immune evasion under Dr. Todd Reynold. After graduating he worked for an additional two years as a lab technician in Dr. Reynolds lab.

He returned to school for a Master's degree at UTK in 2022, where he joined the Burcham lab.